coatings

MDPI

Review

The Preparation of Biomass-Derived Carbon Dots and Its Application Prospect in the Field of Vascular Stent Coating

Huimin Duan [1], Yanchao Wang [1], Zhongna Zhang [1], Ambreen Akram [1,2], Lan Chen [1,*] and Jingan Li [1,*]

[1] School of Materials Science and Engineering & Henan Provine Key Laboratory of Advanced Light Alloys & Key Laboratory of Materials Processing and Mold Technology (Ministry of Education), Zhengzhou University, Zhengzhou 450000, China; duanhuimin@gs.zzu.edu.cn (H.D.); wangyancaho@gs.zzu.edu.cn (Y.W.); zhongna_zhang@gs.zzu.edu.cn (Z.Z.); ambreenakram@gs.zzu.edu.cn (A.A.)

[2] Department of Physics, International Islamic University Islamabad, H-10, Islamabad 44000, Pakistan

* Correspondence: chenlan@zzu.edu.cn (L.C.); lijingan@zzu.edu.cn (J.L.); Tel.: +86-185-3995-6211 (J.L.)

Abstract: Biomass material serves as one of the most advantageous carbon sources for the synthesis of carbon dots (CDs) due to its abundant availability, cost-effectiveness, and environmental sustainability. Biomass-derived carbon dots (B-CDs), which are new zero-dimensional carbon nanomaterials, have presented broad application prospects in the medical field and have become a research focus. In recent years, the death rate caused by vascular diseases has been high, and interventional therapy is one of the important means to treat vascular stenosis. As a material with excellent biocompatibility and fluorescence properties, B-CDs have shown great potential in the field of vascular stents, and their unique properties provide new ideas and possibilities for improving the biocompatibility of vascular stents and realizing real-time tracer diagnosis. This paper reviews the preparation methods, modification techniques, and application prospects of B-CDs in the coating of vascular stents. It discusses current challenges and potential solutions while forecasting future development directions, thereby providing innovative insights and pathways for the research and development of a new generation of vascular stents.

Keywords: biomass material; B-CDs; vascular stent; coating; application prospect

Citation: Duan, H.; Wang, Y.; Zhang, Z.; Akram, A.; Chen, L.; Li, J. The Preparation of Biomass-Derived Carbon Dots and Its Application Prospect in the Field of Vascular Stent Coating. *Coatings* **2024**, *14*, 1432. https://doi.org/10.3390/coatings14111432

Academic Editor: Laura D'Alfonsobreak

Received: 9 October 2024
Revised: 4 November 2024
Accepted: 9 November 2024
Published: 11 November 2024

1. Introduction

In recent years, the morbidity and mortality of cardiovascular disease have remained high, which has become one of the biggest threats to the health of residents [1]. Interventional therapy is one of the important means to treat cardiovascular disease [2]. Among them, stents are commonly used in interventional therapy, but stent implantation is easy to cause thrombosis, in-stent restenosis (ISR) [3], and other problems seriously affecting the quality of life of patients. Therefore, it is of great significance to develop vascular stents with anticoagulation and anti-restenosis functions. B-CDs with excellent fluorescence properties and biocompatibility stand out. Currently, researchers have successfully synthesized carbon-based nanomaterials, including fullerenes, carbon nanotubes, and graphene. However, none of them are ideal fluorescent materials. In 2004, Xu et al. [4] accidentally discovered a new type of fluorescent carbon nanomaterial. They extracted fluorescent carbon nanoparticles from the lysis of carbon nanotubes when purifying single-wall carbon nanotubes by electrophoresis. In 2006, Sun et al. [5] found the substance again with laser ablation of graphite powder and named it carbon dots. CDs are a highly dispersed spherical nanocarbon material with a size of less than 10 nm. Their main components are C, H, and O. They have a highly crystalline sp^2–sp^3 hybrid carbon structure and can be doped with N, P, O, and S elements. The classification of CDs and their structure diagram are shown in Figure 1.

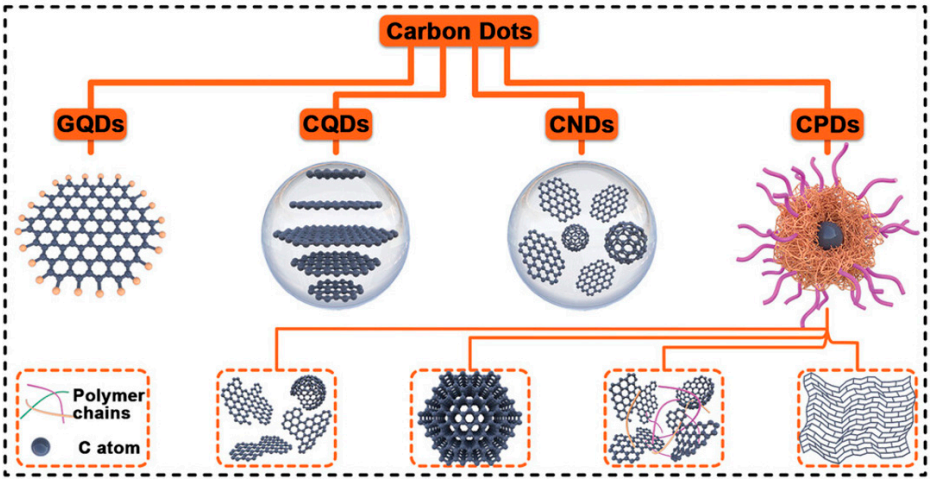

Figure 1. Schematic illustration of the classifications and relevant structures of CDs [6].

Compared with traditional semiconductor quantum dots, the biggest advantages of CDs are low cytotoxicity, high biocompatibility, and good environmental friendliness, which can make up for the shortcomings of semiconductor quantum dots in biomedicine and other fields [7]. In addition, CDs also have the advantages of good water solubility, high chemical stability, controllable photoluminescence, low cost, and a simple synthesis route. Since their discovery, CDs have been widely used in ion probes [8,9], biological imaging [10,11], drug delivery [12], and other fields, as shown in Figure 2. The CDs prepared from biomass precursors have the advantages of a low cost, environmental friendliness, and good biocompatibility. Studies have shown that B-CDs can affect the proliferation, migration, and angiogenesis ability of vascular endothelial cells and have anti-inflammatory and anticoagulation effects [13]. If B-CDs are applied to the surface of vascular stents, perhaps the vascular stents can have the characteristics of promoting endothelialization and antithrombosis. In addition, the fluorescence properties of B-CDs enable them to be used for real-time imaging and monitoring of vascular stents. B-CDs can also serve as drug carriers to achieve targeted drug delivery and sustained release, thereby improving the therapeutic effect. In the future, by optimizing the properties and surface functionalization of B-CDs, it is expected to further enhance their promoting effect on vascular tissue regeneration, accelerate the repair process after vascular injury, reduce the risks of vascular restenosis and thrombosis, and provide a new approach for the treatment of cardiovascular diseases.

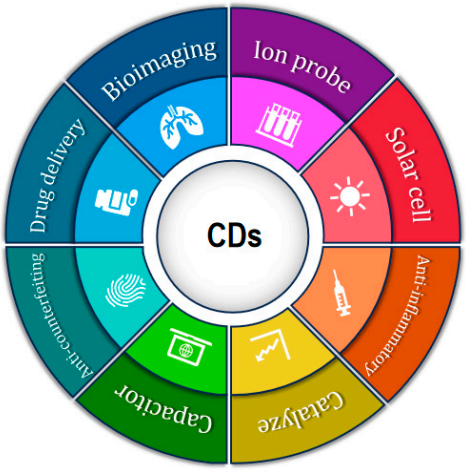

Figure 2. Application field of CDs.

However, there has not been any research on combining B-CDs with vascular stents yet. The preparation and modification methods of B-CDs will be reviewed in this paper to provide a theoretical basis and reference for further optimization of the preparation process and preparation of excellent quality B-CDs. In addition, the application prospects and challenges of B-CDs in the coating of vascular stents were preliminarily discussed in this paper, and the possible development direction of B-CDs in the field of vascular stents in the future was prospected, providing new ideas for the development of a new generation of vascular stents.

2. Preparation of B-CDs

2.1. Precursors

CD precursors refer to the main components used in the production of CDs, and biomass stands out as a green, cheap, readily available, sustainable, and renewable carbon source. Natural polymers, plants, agricultural wastes, and biomass residues can be used as precursors of B-CDs. The selection of suitable biomass raw materials as the precursor of B-CDs has a profound impact on the performance of B-CDs [14]. From fluorescence intensity to structural diversity to cost-effectiveness and environmental friendliness, the choice in raw materials directly determines the ultimate application potential of B-CDs. The functional groups in the precursors play a significant role in the fluorescence characteristics of the synthesized B-CDs, which can significantly change the fluorescence characteristics of B-CDs. For instance, the incorporation of nitrogen-containing precursors can enhance both the fluorescence intensity and stability of B-CDs, as the introduction of nitrogen modifies the electronic structure and improves light absorption and fluorescence emission [15–17]. Plant leaves are able to generate B-CDs without the need for any passivating agents, reducing agents, oxidants, or organic solvents, enabling green production [18]. The structure of B-CDs can be amorphous, crystalline, or mixed, depending on the selected synthesis method and precursor material. Different raw materials lead to different synthetic paths, which in turn affect the final structure of B-CDs. The higher reaction temperature usually promotes the carbonization degree of the carbon source, reduces the size of B-CDs, increases the crystallinity, and affects the performance of B-CDs [19–22]. Conventional CD preparation methods often rely on fossil fuels or harmful chemicals, while biomass precursors are usually cheaper and easier to obtain, and the synthesis process of B-CDs is straightforward and environmentally friendly [23]. The effective use of biomass materials can minimize the emission of these noxious substances [24]. Finally, the impurity content is also a significant element affecting the properties of B-CDs. No matter which preparation method is used, impurities are inevitably introduced, which may include uncarbonized precursors, polymers, or carbon particles. B-CDs solution can be purified by centrifugation, dialysis, filtration, and other methods to remove impurities that may be introduced in the preparation process [25].

Since the discovery of CDs, numerous reports on the preparation of B-CDs from biomass have emerged. B-CDs synthesized from tea [26], vegetables [27], and fruit pits [28] have been successfully applied in various fields. Recently, traditional Chinese medicines (TCMs) have attracted wide attention due to their unique medicinal value. TCM-CDs prepared by TCM have lower toxicity and are more suitable for in vivo application [29]. Many TCMs usually contain a variety of organic compounds such as alkaloids, flavonoids, terpenoids, and polysaccharides, which can provide abundant carbon sources and heteroatom doping for the formation of B-CDs during pyrolysis or hydrothermal treatment, thus giving B-CDs unique properties [30]. TCM itself has certain biological activities and medicinal effects, and TCM-CDs may retain part of the activity of the original components of traditional Chinese medicine, thus presenting diversified mechanisms of action so that it can be applied to hemostasis [31], anti-inflammatory, hemostasis [32], anticancer [33], antibacterial, and repair blood–brain barrier (BBB) damage. Vibhute, A et al. [34] synthesized B-CDs from Cherimoya leaves by the hydrothermal method, which showed good anti-inflammatory and antibacterial properties. B-CDs prepared with peach kernel and

safflower as the precursor system can improve the nerve function of mice after nerve injury and traumatic brain injury, reduce brain edema, and reduce blood–brain barrier permeability after injection through the tail vein. The B-CDs can also inhibit the expression of inflammatory factors such as IL-1, IL-6, and TNF-α, which have a good anti-inflammatory effect [35]. Bhattacharya, T et al. [36] prepared undoped and sulfur-doped B-CDs using dried Gromwell roots as precursors. Research has proven that both of these B-CDs have good antibacterial activity, and the sulfur-doped B-CDs enhance catalytic activity as well as have better antioxidant activity and free-radical scavenging ability. According to Chinese pharmaceutical research and clinical research, salvia miltiorrhiza, safflower, Chuanxiong, notoginseng, and other TCMs have the effects of facilitating blood circulation, eliminating blood stasis, inhibiting platelet aggregation, antithrombus, and anticoagulation. B-CDs prepared by it may inherit or enhance these characteristics so that they have potential application value in the field of vascular stents; integrating conventional medical wisdom with contemporary science and technology can lead to innovative research concepts and new areas of application.

In summary, the choice in precursors exerts a great impact on the properties of B-CDs. Suitable precursors contribute to the synthesis of CDs with good biocompatibility and reduce irritation to vascular tissue. If the precursor is properly selected, the prepared B-CDs can enhance the stability of the scaffold coating and ensure its long-term function in the complex environment in vivo. Specific precursors enable B-CDs to possess specific optical properties, facilitating the monitoring of the position and condition of the scaffold. Good precursors can also regulate the surface chemistry of B-CDs, promote the adhesion and growth of endothelial cells on the scaffold surface, and accelerate the repair of vascular intima. The selection of B-CDs precursors is very important for their application in the coating of vascular stents, which directly affects the performance, biocompatibility, and clinical application effect of stents.

2.2. Preparation

Studies have shown that natural biomass, including plants, animals, and microorganisms, can be used as precursors for the synthesis of B-CDs. The growth of CDs usually starts from nucleation. During the preparation process, precursor molecules form small crystal nuclei through chemical reactions under certain conditions such as the temperature, pressure, and solvent. After nucleation, the carbon nuclei will continuously grow by absorbing the surrounding precursor molecules or other active substances [37]. According to the formation mechanism and reaction conditions of B-CDs, the preparation methods can be divided into the "Top-Down" method and the "Bottom-Up" method. The two synthesis routes of CDs are shown in Figure 3. The synthesis method, particle size, lattice spacing, and quantum yield (QY) of B-CDs from different precursors are shown in Table 1.

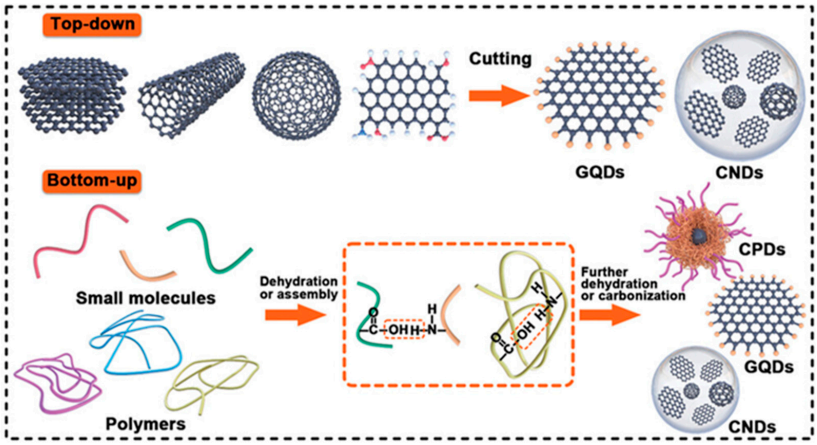

Figure 3. Schematic illustration of two classical synthesis routes for CDs: top-down method and bottom-up method [6].

2.2.1. "Top-Down" Method

The "Top-down" method is a method that strips or breaks large carbon materials to form small fluorescent carbon nanoparticles and then modifies their surface to improve their performance. It is inclined to B-CDs with large production volumes, but the size and shape of B-CDs are difficult to control, the fluorescence intensity is not high, and the operation is complicated. The following details several "top-down" methods of B-CDs synthesis and their merits and demerits.

The arc discharge method is the earliest method to prepare CDs. This method is to vaporize and decompose carbon materials in an inert gas environment by arc discharge between two electrodes to prepare CDs. Xu et al. [4] extracted fluorescent carbon nanoparticles by electrophoresis when purifying single-wall carbon nanotubes, which was the first time CDs were prepared. Biazar, N et al. [38] prepared CDs by applying arc discharge between two graphite electrodes in water using the liquid DC arc discharge method. The CDs/TiO_2 nanomaterial prepared by coupling CDs with TiO_2 particles showed great photocatalytic activity in the visible light band. The preparation of CDs by the arc discharge method is simple and relatively efficient. By adjusting arc discharge parameters, such as current, voltage, discharge time, inert gas type, and flow rate, the size, structure, and performance of CDs can be regulated to a certain extent, which provides a certain space for studying the properties of CDs and optimizing the preparation process. However, this method has high requirements for equipment, a low yield of CDs fluorescence quantum, and certain safety risks.

The laser ablation method is the use of high-intensity laser irradiation of a carbon target so that it evaporates and decomposes, and carbon nanoparticles are peeled off from the carbon target to produce CDs. Kaczmarek, A et al. [39] successfully prepared CDs with obvious lattice stripes by pulsed laser ablation of graphite targets immersed in polyethyleneimine (PEI) or ethylenediamine (EDA) solutions, respectively. Isnaeni et al. [40] dissolved 0.01 g coconut fiber toner in 1 mL toluene and used three laser sources with different wavelengths of 355 nm, 532 nm, and 1064 nm to laser ablate the mixed solution for 1 h and 2 h, respectively, and finally removed the non-ablated powder during the ablation process by centrifugation. They found that there may be a quantum confinement effect in B-CDs samples, increasing the ablative wavelength can produce higher emission intensity B-CDs, and extending the ablative time can produce better B-CDs. The laser ablation method can control the synthesis condition precisely, but it also has the problem of a low yield. It does not depend on hazardous chemicals and utilizes relatively low energy, positioning it as a promising candidate for sustainable synthesis [41].

The electrochemical oxidation method is under a certain potential, using carbon material as the working electrode, after the electrolyte is oxidized in the anode, carbon nanoparticles are peeled off from the working electrode, and then through surface passivation treatment, carbon nanoparticles are converted into CDs with fluorescence properties. The aqueous solution was used as an electrolyte. Xu et al. [42] carried out electrochemical oxidation of the screen-printed carbon electrode, and the prepared CDs showed obvious photoluminescence. The cytotoxicity of CDs was detected by the MTT method, and it was found that HeLa cell viability was negatively correlated with CDs concentration, but the overall cell survival rate was higher than 70%, which proved that the synthesized CDs had low toxicity. Li et al. [43] used carbonized corncob with a three-dimensional porous structure as the anode, platinum wire as the cathode, and KOH aqueous solution as the electrolyte to successfully prepare B-CDs dispersed in the electrolyte by the electrochemical oxidation method and then separated and purified the B-CDs by filtration dialysis and other steps. The B-CDs/rGO (reduced graphene oxide) aerogel composites were prepared by combining them with rGO. The composites not only improved the poor electrical conductivity of the B-CDs but also increased the sodium storage capacity of the composite aerogel, and the presence of the B-CDs effectively inhibited the self-stacking of rGO. The electrochemical oxidation method has the advantages of simple instruments, convenient

operation, and a low cost and can adjust the size and luminescence properties of B-CDs by changing the current intensity. The preparation cost is low, while the product has a low QY.

2.2.2. "Bottom-Up" Method

Among them, the "bottom-up" method is mainly used to carbonize and assemble molecular precursors and synthesize CDs through combustion or heat treatment. This method can control the size and shape of CDs more effectively, but the process is more complicated and time-consuming. The fluorescence intensity and QY can be improved by doping heteroatoms. The following details several methods of "bottom-up" CDs synthesis and their advantages and disadvantages.

The hydrothermal method is the most frequently used one for synthesizing B-CDs. For the preparation of B-CDs by the hydrothermal method, the water solubility of the precursor is an important consideration. Precursors with good water solubility, such as glucose and some amino acids, are more likely to be evenly dispersed in the hydrothermal reaction, which is conducive to the formation of B-CDs. Using deionized water as a solvent, under high-temperature and high-pressure conditions, the organic molecules in biomass undergo self-polymerization or mutual polymerization in the reaction kettle to form various cross-linked structures, and then B-CDs are prepared by carbonization. Zheng et al. [44] successfully extracted highly fluorescent nitrogen-doped B-CDs from Panax notoginseng by the hydrothermal method for bioimaging and highly selective detection of Cr^{6+}. Using cucumber skin as a carbon source, B-CDs prepared by the hydrothermal method were integrated into the fibrin clot network in a concentration-dependent manner. Streptokinase triggered clot dissolution and B-CDs release, and streptokinase could be detected by fluorescence with high selectivity [45]. This method is easy to operate, low cost, and easily modifies the surface of B-CDs. Although the preparation period of this method is long, the synthesized B-CDs usually contain some hydrophilic functional groups, which can not only improve the biocompatibility of the B-CDs themselves but also provide abundant reaction sites for the surface of B-CDs, and various functional groups can be introduced through chemical reactions to achieve functional modification of B-CDs.

The solvothermal method is an advancement derived from the hydrothermal method. Different from the hydrothermal method, the solvothermal method uses organic matter or non-aqueous solvents as solvents under high temperatures and pressure. Under solvothermal conditions, the interdependence of solvent density, viscosity, and dispersion significantly alters their properties compared to normal conditions. This environment greatly enhances the dissolution, dispersion processes, and chemical reactivity of the reactants, which are typically in solid form. Liu et al. [46] extracted fresh mulberry leaf juice with ethanol and reacted at 150 °C to produce red B-CDs with hydrophobic groups. After feeding the B-CDs to silkworms, fluorescent silk with good biocompatibility and mechanical properties was successfully obtained. Chen et al. [47] used gallic acid and o-phthalaldehyde as raw materials and acetone, methanol, and DMF (dimethylformamide) as solvents, respectively. Through the aldol condensation reaction, they prepared B-CDs with orange-red, green, and blue luminescence, which have good optical and thermal stabilities. It was found that the reaction solvent directly affected the carbonization process of the late precursor, changed the size of the sp^2 conjugated domain, and directly led to the difference in the fluorescence color of B-CDs. Solvothermal methods can be performed at relatively low temperatures, thus reducing energy consumption and equipment costs. However, the response procedure demands the use of organic solvents, which may pollute the surroundings to some extent.

The microwave-assisted method uses biomass as a precursor. Under the action of microwaves, the carbon chains in biomass molecules begin to break, recombine, and carbonize. As the temperature rises and the reaction proceeds, small molecular carbon aggregates gradually form, and these aggregates continue to undergo structural adjustment and surface modification, and eventually form B-CDs with nanoscale. Liu et al. [48] adopted the microwave-assisted polyol one-step method, using 1 mL 30% sucrose as a carbon source,

3 mL diethylene glycol as a reaction medium, and adding 200 µL concentrated sulfuric acid as a catalyst for sucrose dehydration and carbonization; B-CDs could be prepared within 1 min of microwave irradiation. The prepared B-CDs had low cytotoxicity, green photoluminescence, and obvious lattice fringes, indicating that they had a high degree of graphitization. Tabaraki, R et al. [49] prepared nitrogen-doped B-CDs using citric acid as a precursor and potassium cyanide as a nitrogen source by the microwave-assisted method. The B-CDs were used to detect the concentration of Pb^{2+}. Studies have shown that, in comparison with the old-fashioned hydrothermal method, microwave-assisted preparation of B-CDs has higher self-doped nitrogen, and as a result, the position of the fluorescence emission peak or absorption peak of the B-CDs moves to the long-wavelength direction, that is, redshifts [50]. The microwave-assisted method has a short reaction time and high efficiency, but the particle size of the CDs is not easy to control, and the preparation process has high requirements on the equipment, and attention needs to be paid to the uniformity and safety of microwave radiation.

Pyrolysis is the process of heating the precursor to a high temperature in an inert atmosphere. The chemical bonds of macromolecular organic compounds within biomass (such as cellulose, hemicellulose, lignin, etc.) are broken. After a series of complex chemical reactions, including dehydration, decarboxylation, and polymerization, a nanoscale carbon core structure is gradually formed. With the progress of the reaction, these carbon nuclei continue to grow and aggregate, while the surface will form a variety of functional groups, such as hydroxyl, carboxyl, carbonyl, and so on, and finally form B-CDs with unique optical properties. Chen et al. [51] adopted the method of carbonized sucrose oleate to rapidly synthesize CDs under magnetic stirring at 215 °C. The B-CDs synthesized by this method are monodisperse and amorphous, and their photoluminescence intensity remains almost unchanged under the conditions of ultraviolet excitation for a short time and long-term storage within the pH range of 2~8. The pyrolysis method has the characteristics of simple operation, short reaction time, and strong controllability. However, the purity of the prepared B-CDs is relatively low, and some harmful gases and wastes may be generated during the pyrolysis process, which may cause environmental pollution.

Table 1. Synthesis method, particle size, lattice spacing, and QY of B-CDs from different precursors.

Precursors	Specific Type	Synthesis Method	Particle Size (nm)	Lattice Spacing (nm)	QY (%)	Applications	References
Natural polymer	Biomass bacterial cellulose	Hydrothermal method	1~5	0.21~0.32	-	Highly sensitive bacterial detection	[52]
	Collagen waste	Hydrothermal method	1.2~9	0.32	3.5~7.5	Cell imaging	[53]
	Microcrystalline cellulose	Hydrothermal method	1~7	0.26	28.4	Fe^{2+} detection	[54]
	Chitosan/ ethylenediamine	MW-assisted method	15	-	1.16~7.07	Fluorescence imaging of Candida albicans	[55]
	Hyaluronic acid	MW-assisted method	7	-	7~12	Dual active targeting and imaging of HeLa cancer cells	[56]
Plants and their extracts	Spent tea leaves	Hydrothermal method	2.0~5.0	2	-	Supercapacitor electrode	[57]
	Citric acid/piperazine	MW-assisted method	3.2~7.8	0.22~0.3	-	LED and fingerprint detection	[20]
	Osmanthus	Hydrothermal method	3.6	0.21	-	Cell imaging and NIR photothermal therapy	[58]
	Pivalic acid/gelatine	Pyrolysis method	2.5	-	22.4	Drug delivery and antioxidant	[59]
	Citric acid/zinc chloride	MW-assisted method	2~4	-	51	CDs with controllable emission characteristics were prepared	[60]

Table 1. *Cont.*

Precursors	Specific Type	Synthesis Method	Particle Size (nm)	Lattice Spacing (nm)	QY (%)	Applications	References
Agricultural waste	Rice husk	Hydrothermal method	3.6~7.1	0.22~0.24	54	Cellular imaging and drug delivery	[61]
	Charcoal	Laser ablation method	2~10	-	-	Optical sensing and biological imaging	[62]
	Peanut shell/ citric acid	Pyrolysis method	2~13	-	21	Selective detection of Cu^{2+}	[63]
	Green tea residue	Hydrothermal method	2.2	0.3	10.4	Detection of heavy metal ions in food	[64]
	Corncobs	Electrochemical oxidation method	1~4	-	10.16	Na^{+} batteries	[43]
Biomass residue	Cow milk	Hydrothermal method	7~8	-	38	Sn^{2+} detection	[65]
	Cow milk/ phosphoric acid	Hydrothermal method	10	-	17.15	Au^{3+} detection	[66]
	Orange peel	MW-assisted method	4.2	0.26	16.2	Detection of Escherichia coli in milk	[67]
	Lemon peel	Hydrothermal method	1.5~5.0	0.36	-	Tumor cell detection	[68]
	Hawthorn	Hydrothermal method	3.17	0.2	22.96	Rapid determination of chlortetracycline in pork samples	[69]

2.3. Optical Properties

B-CDs have good photoluminescence properties. They usually exhibit strong absorption in the ultraviolet region (200~400 nm), and the absorption band can be attributed to the π–π* transition of carbon–carbon double bonds or the n–π* transition of carbon–oxygen and carbon–nitrogen bonds [70]. TEM is a commonly used method for characterizing the size and morphology of B-CDs. The size of most B-CDs is below 10 nm. The quantum confinement effect causes the change in the electron transition energy of B-CDs, thus generating a luminescence phenomenon. This quantum confinement effect not only influences the intensity of fluorescence but also affects its spectral characteristics, providing researchers with an additional means to adjust the fluorescence properties [71]. For example, due to the stronger quantum confinement effect, smaller-sized B-CDs have their luminescence wavelength shifted towards the blue light direction. Singh, V et al. [72] used beetroot as a precursor to prepare blue and green fluorescent B-CDs with an average diameter of 5 nm and 8 nm, respectively, by hydrothermal treatment and orthophosphoric acid treatment. In addition, the surface state, doping elements, and synthesis conditions of B-CDs can also adjust their emission wavelength, enabling B-CDs to exhibit different fluorescence colors and fluorescence intensities [73]. Zhou et al. [74] synthesized a kind of blue B-CDs using hydrogenated rosin as a precursor by the hydrothermal method. These B-CDs can be used as a fluorescent probe for Fe^{3+} and for bio-imaging. The researchers found that the fluorescence intensity of the B-CDs increased with the increase in the ratio by adjusting the proportion of glycerol and water. Some researchers prepared B-CDs using three different agricultural wastes as precursors and found that the luminescence wavelength of these B-CDs had a redshift, and the QY also increased with the increase in the synthesis temperature. Some B-CDs have room-temperature phosphorescence characteristics, which are generated by two key processes: intersystem crossing from the lowest excited state to the triplet state and radiative transition from the lowest excited triplet state to the ground state. Zhao et al. [75] prepared silicon-doped B-CDs with room-temperature phosphorescence and then chemically cross-linked them with carboxymethyl cellulose to successfully prepare a gel. Compared with the individual B-CDs, this gel has a longer phosphorescence lifetime and greater phosphorescence intensity and can be used for luminescent anti-counterfeiting materials. Compared with other fluorescent carbon nanomaterials, such as traditional

fullerenes, carbon nanotubes, and graphene, they have good luminous stability in common and have applications in catalysis, sensing, and biomedicine [76–78]. However, B-CDs have better biocompatibility. The abundant functional groups on the surface of B-CDs endow them with high surface reactivity. B-CDs usually have relatively irregular crystal structures with more defects. Fullerenes, carbon nanotubes, and graphene have ordered crystal structures and better electrical conductivity. The thermal conductivity and thermal stability of carbon nanotubes and graphene are also far superior to those of B-CDs.

2.4. Modification Methods

By changing the biomass raw materials used in the synthesis process or through post-treatment methods, the surface chemical properties of CDs can be adjusted to meet different application requirements [79]. Doping is a general and convenient functionalization technique for modifying the inherent structure of CDs by inserting heteroatoms into the CD structure, while surface modification is a functionalization method guided by application requirements. Both can effectively regulate the chemical, optical, and electrical properties of CDs to meet different application requirements.

2.4.1. Heteroatom Doping

Doping heteroatoms such as nitrogen, phosphorus, and sulfur into B-CDs can change the electronic structure and energy band structure of B-CDs, thereby affecting their optical, electrical, catalytic properties, etc. Purposeful regulation of B-CDs is conducive to promoting their effective applications. Biomass itself usually contains multiple elements such as C, N, and O, which is helpful for naturally introducing heteroatoms during the synthesis process, changing the physical or chemical properties of B-CDs and thus regulating the performance of B-CDs. Research by Liu et al. [80] has proven that exogenous nitrogen doping can modify B-CDs more effectively compared to biomass self-doping, endowing them with more nitrogen-containing functional groups, and a slightly elevated reaction temperature can increase the doping level.

Heteroatom doping is capable of enhancing the optical properties of B-CDs [81]. Nitrogen doping can increase the fluorescence intensity of B-CDs, make the fluorescence emission peak redshift or blue shift, broaden the fluorescence emission range of B-CDs, and help to obtain B-CDs with specific fluorescence characteristics to meet the needs of different optical applications [50,82]. Olla, C et al. [83] compared the "bare carbon point" prepared with citric acid as the precursor system and nitrogen-doped B-CDs and found that the QY of the nitrogen-doped carbon point was as high as 9.6%, much higher than that of undoped samples. Oh, GH et al. [84] prepared B-CDs using citric acid as a carbon source, urea as a nitrogen source, and DMF as a solvent by the solvothermal method at 200 °C for 12 h. The B-CDs were added to ethyl acetate, isopropyl alcohol, and acetone to obtain blue, green, and red emission B-CDs, respectively. Through the incorporation of nitrogen, the luminescence wavelength of B-CDs can be adjusted, thereby achieving different colors of luminescence. This may be because the introduction of nitrogen atoms changes the electronic structure and energy-level distribution of B-CDs, thus having an impact on its fluorescence emission wavelength, intensity, QY, etc. [85,86]. Heteroatom doping can regulate the chemical properties on the surface of B-CDs. The doping of heteroatoms will introduce more active sites on the surface of B-CDs, such as nitrogen-containing groups (such as amino group, pyridine nitrogen, etc.) and oxygen-containing groups (such as carboxyl group, hydroxyl group, etc.), which can enhance the interaction between B-CDs and other substances [87]. Heteroatom doping is able to enhance the electrochemical performance of B-CDs. Heteroatom doping can introduce additional energy levels, which can be located between the conduction band and the valence band, thus decreasing the band gap. The decrease in the band gap facilitates the jump of electrons from the valence band to the conduction band, thereby enhancing the conductivity of the material. This phenomenon is particularly evident in nitrogen-doped B-CDs, where the nitrogen atoms provide additional electrons, increasing the concentration of charge carriers and thus improving electrical

conductivity [88,89]. In addition, phosphorus doping has also been found to effectively increase electron concentration and provide additional electrochemically active sites, promoting the improvement of electrical conductivity [90]. Heteroatom doping can broaden the application of B-CDs in the medical field. Heteroatom doping can improve the biocompatibility and targeting of B-CDs, which makes it more widely used in bioimaging [91], drug delivery [92], biosensing [93], and other fields. Heteroatom doping increases the surface-active site of B-CDs, thus enhancing its adsorption capacity to drug molecules. For example, Shi et al. [94] prepared B-CDs with a one-step carbonization method using wheat straw as a single precursor. Then, H_3BO_3 and $Na_2B_4O_7$ were mixed with B-CDs and reacted at 200 °C for 10 h to obtain boron-doped B-CDs and finally coated with isophthalic acid (IPA). B-CDs@IPA has been successfully applied to live cell imaging and detection of Cu^{2+} content. B-CDs@IPA solid powder can display different solid fluorescence under different wavelength ultraviolet irradiation. Darwish, HW et al. [59] used valeric acid and natural gelatin as precursors to prepare nitrogen-doped B-CDs with good cellular compatibility by pyrolysis and loaded the anticancer drug molecule doxorubicin hydrochloride into B-CDs. It was found that B-CDs have a strong antioxidant activity (>80%) and act as a nanoparticle carrier, and the loaded doxorubicin hydrochloride release is pH-dependent.

2.4.2. Surface Modification

Surface modification refers to the modification of the surface of a material by chemical or physical methods in order to change its surface properties and functions. For B-CDs, surface modification can include changing its size, shape, adding functional groups, doping of heteroatoms, etc. Small and uniform B-CDs usually have good photoluminescence properties, capable of emitting intense fluorescence at specific wavelengths. Studies have shown that using different surface modification methods, such as amide coupling reactions, can effectively change the shape of B-CDs, making them more uniform and regular [95]. Doping can change the surface polarity and water solubility of B-CDs [96]. Nitrogen doping and phosphorus doping can increase the number of polar functional groups such as the amino (-NH_2), pyridine-N, and phosphate group (-PO_4) on the surface, improve the hydrophilicity of B-CDs, enhance their dispersion in water, and then improve the surface wettability of B-CDs. Or by introducing hydrophilic groups, biocompatible polymers, or specific biomolecules, the surface properties of B-CDs can be improved, their surface energy can be reduced, and non-specific interactions with biological tissues can be reduced. Polyethylene glycol (PEG) and polyethylenimine are often used as passivating agents to modify the surface of B-CDs. Sangjan, A [97] et al. prepared B-CDs containing a large number of hydroxyl groups by using an oil palm empty fruit cluster as a carbon source and PEG as a passivating agent in a one-pot hydrothermal method. The hydroxyl group of PEG was successfully grafted onto the surface of B-CDs, which improved the hydrophilicity of the B-CDs. This is very important for the application of B-CDs in biomedicine, environmental monitoring, and other fields so that B-CDs can better interact with biological systems or environmental media. The optical properties of B-CDs are highly relevant to their surface state. Their luminescent properties, such as luminescent intensity, luminescent wavelength, and QY, can be adjusted by surface modification. Javeria, H et al. [63] prepared B-CDs by carbonizing peanut shells and then pyrolyzed B-CDs with citric acid at 400 °C for 4 h. The citric acid combined with the oxygen-containing functional group on the surface of B-CDs overcame the defect site, successfully passivated the B-CDs, and improved the QY. Zhang et al. [69] prepared B-CDs from hawthorn powder and diethylenetriamine (DETA) by the one-step hydrothermal method. As the ratio of DETA and Hawthorn powder increased, the fluorescence intensity of B-CDs first increased and then decreased. The surface modification exerts a profound influence on the material properties of B-CDs. As research progresses further, the future surface modification technology will further promote the application of B-CDs in various fields and open up new directions for the development of new materials.

3. The Coating Technology for Vascular Stents and Its Surfaces

3.1. Evolution of Vascular Stent

A vascular stent is a kind of medical device used to treat vascular stenosis or occlusion. It is mainly made of metal or polymer material. It is an internal stent inserted in the diseased segment (narrow occlusive segment of blood vessels) on the basis of luminal balloon expansion and formation and belongs to one of the vascular interventional instruments. Vascular stents are mainly divided into coronary stents, intracranial stents, and peripheral vascular stents. Its main purpose is to support the narrow-occluded blood vessels, reduce the elastic retraction and remolding of blood vessels, and keep the lumen blood flow unobstructed. The diameter of the stent is usually 2~6 mm, the wall thickness is 0.1~0.2 mm, and the length has different specifications according to the location of the lesion, ranging from a few millimeters to tens of millimeters. However, studies have proven that the length of stents is linearly correlated with the incidence of restenosis, and the implantation of long stents is accompanied by an increase in the incidence of restenosis [98]. Vascular stents can be used to treat a variety of vascular diseases, such as atherosclerosis [99] and coronary artery stenosis. Coronary atherosclerosis is the main cause of coronary artery stenosis [100]. Figure 4a shows the phenomenon of coronary artery stenosis caused by the blockage of the coronary artery by fat or cholesterol accumulation. Percutaneous transluminal coronary angioplasty (PTCA) represents the primary interventional procedure for the management of coronary artery stenosis. However, restenosis is a major problem it faces. The processes of PTCA and restenosis are shown in Figure 4b. Percutaneous coronary intervention (PCI) with stent deployment, as shown in Figure 4c, is the main form of current treatment.

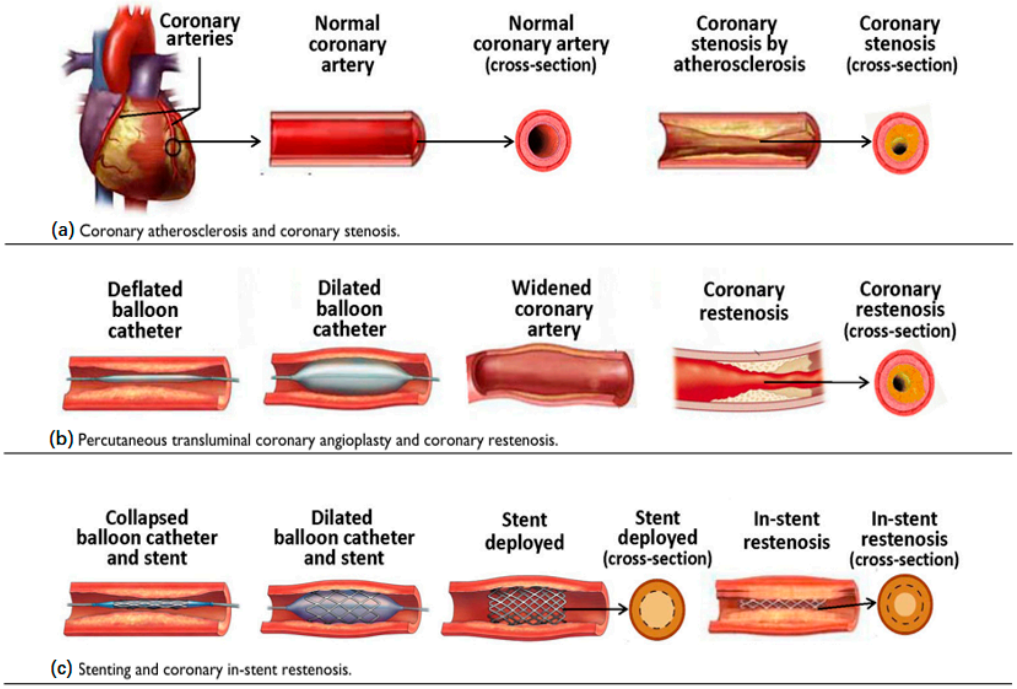

Figure 4. (**a**) Coronary artery atherosclerosis and stenosis; (**b**) percutaneous transluminal coronary angioplasty and coronary artery restenosis; (**c**) stenting and coronary in-stent restenosis [101].

The wound caused by vascular stent implantation is small, the surgical risk is low, and the impact on the patient's body is relatively small. As shown in Figure 4c, after the vascular stent is implanted in the body, it goes through two stages. Even strenuous activities, sudden postural changes, severe coughing, etc. are unlikely to cause displacement. Therefore, there is no need to worry that vascular stent implantation will significantly affect normal life. Under the action of the human body's self-repair function, platelets with the hemostatic function will gather at the site where the vascular stent is placed, which is likely to cause restenosis of blood vessels [102]. Consequently, following the implantation of vascular

stents, patients are required to adhere to a regimen of antiplatelet medications (such as aspirin, clopidogrel, etc.) for a long time to maintain the patency within the stents, but this also increases the risk of bleeding in the body. Clopidogrel can prolong the recovery of platelet reactivity and inhibit platelet aggregation, but it still has significant inter-individual variability in clinical treatment. Anemia may occur in some people due to a reduced response to the drug; in addition, some people may experience massive bleeding due to an excessive response to the drug. Moreover, there is also the possibility of restenosis of the stent [103,104]. After the implantation of a vascular stent, while propping open the blood vessel, it also damages the vascular endothelium, leading to inflammation, proliferation of vascular smooth muscle cells, and neointima formation [105]. All of these will lead to the occurrence of stent restenosis, as shown in Figure 4c, and eventually lead to an increase in the mortality rate of postoperative patients [3,106].

The development of vascular stents has gone through several important stages. Its first revolution occurred in the 1990s when the bare metal stent (BMS) was born. Sigwart et al. [107] were the first to apply a stent made of knitted stainless-steel metal in clinical practice and completed the world's first coronary artery bare metal stent implantation. However, after stent dilation, vascular damage causes an inflammatory response. The probability of IRS after BMS implantation is as high as 20%~30% [108,109]. In order to solve the problem of ISR in the later stage, the attempt to cover the surface of the metal stent with an anti-proliferative drug coating successfully reduced the restenosis rate in the stent to less than 10%, injecting new vitality into PCI treatment [110]. It was the first generation of drug-eluting stents (DESs) and the second revolution in interventional cardiology. The drug coatings of the first generation of DES were mainly paclitaxel and rapamycin, which inhibited smooth muscle cell proliferation while also inhibiting vascular endothelial repair, easily causing late stent thrombosis [111]. To address the above challenges, Fu et al. [112] developed an integrated hydrogel (Cur-NO-Gel) that regulates arterial remodeling. This integrated hydrogel employs a three-pronged approach to combat stenosis post-angioplasty, as shown in Figure 5. Cur-NO-Gel combines the vasodilator effect of NO with curcumin's function of inhibiting neointima and protecting the endothelium to inhibit post-angioplasty vascular stenosis in three ways (promoting endothelial cell regeneration, inhibiting intima hyperplasia, and improving contractile remodeling). The new generation of DES has improved the drug-carrying coating, which includes three kinds of biocompatible polymer coating, degradable polymer coating, and non-polymer coating. The new generation DES improves the late clinical prognosis of patients and is the mainstream device in PCI therapy. However, the implantation of permanent foreign bodies may have the possibility of in-stent restenosis ISR [113], and the occurrence of late restenosis after long-term implantation is thought to be related to the degradation of drug carriers on the stent, so the third-generation biodegradable vascular stent (BVS) was introduced for the treatment of vascular diseases. To address complications of DES, this type of stent is usually made of biodegradable materials such as polylactic acid, polyglycolic acid, and magnesium-based and iron-based alloys [114]. It can avoid the long-term complications potentially induced by the long stay of vascular stents in the body. Moreover, the biodegradable materials used usually have good biocompatibility, which reduces the irritation to the blood vessel wall and the inflammatory response and is beneficial to the long-term health of blood vessels. However, this type of vascular stent also faces some challenges. First of all, in comparison with metal stents, the mechanical strength of biodegradable vascular stent (BVS) may be inferior to that of metal stents, and its early degradation might result in blood vessel collapse. Secondly, the degradation rate of the BVS needs to match the blood vessel repair process, etc. [114,115].

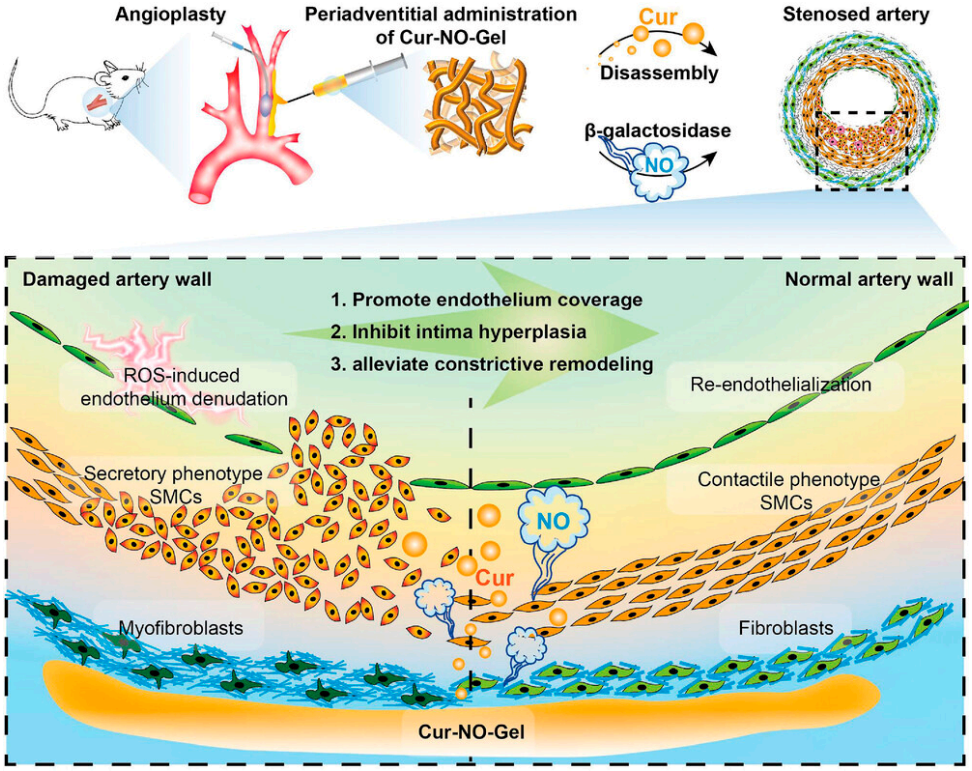

Figure 5. Schematic description of Cur-NO-Gel [112]. Cur-NO-Gel, administered periadventitially, possesses the unique ability for sustained Cur release and on-demand liberation of NO.

3.2. Coating Technology of Vascular Stent

Vascular stents have gone through three development stages, mainly reflected in improvements in two key aspects. One is the optimization and innovation of the stent material itself, and the other is the innovation and development of the stent coating. Firstly, the drugs in the DES directly diffuse into the blood vessel wall, and targeted drug delivery improves the utilization rate of drugs. However, after the drugs are released into the blood flow, they directly contact the endothelial cells inside and downstream of the stent, affecting the proliferation and migration speed of these cells [116]. Secondly, the coating can improve the biocompatibility between the stent and the blood vessel wall, decreasing the risk of inflammatory reactions and thrombosis formation. For example, Sun et al. [117] combined sulfonated hyaluronic acid and metal–organic framework copper to form a composite coating with anticoagulation, anti-inflammatory, and endothelialization properties on the surface of magnesium alloy vascular scaffolds. Currently, there is still much room for improvement in aspects such as the perfect degree of blood compatibility of vascular stents, the precision of drug-controlled release, and the guarantee of long-term stability [118]. After stent implantation, both overgrowth and hypo-endothelialization of endothelial cells may cause restenosis and thrombosis, and how to achieve the ideal balance of the endothelialization process is still a hot research topic and a challenging problem [119,120]. It is a complex problem to develop a new type of vascular stent with the function of integrated diagnosis and treatment and to effectively integrate functions, such as antithrombotic, anti-inflammatory, and endothelialization, into one coating and make them work in synergy.

B-CDs may be a way out of this dilemma. B-CDs with low toxicity and good biocompatibility have mild interaction with vascular tissue, do not easily cause serious immune response or inflammation, can reduce the stimulation and damage to the vascular wall, and help reduce some complications after stent implantation [121]. By surface modification or with drug loading [122], B-CDs can confer new properties on vascular stents. For example, we can graft anticoagulants or platelet inhibitors onto the surface of B-CDs

or apply modified B-CDs with anticoagulant properties to the coating of vascular stents. This can effectively prevent blood from coagulating on the surface of the stent and is of great significance for preventing thrombosis after stent implantation. In addition, the size, surface charge, and optical properties of B-CDs can be controlled by synthetic methods and surface modification [123]. When fluorescent B-CDs are applied to the coating of vascular stents, the small-size B-CDs can clearly display the fine structure of the stent, thus providing high-resolution imaging to realize the visualization of the position, shape, and integrity of the vascular stent in vivo, which is convenient for timely detection of potential problems and intervention measures [124,125]. Nanoscale B-CDs can also be combined with other materials to construct composite scaffold coating materials with higher properties, which will bring new breakthroughs in the treatment of vascular diseases. B-CDs have a broad application prospect in vascular stent coating, which is expected to improve biocompatibility, antithrombotic properties and promote endothelialization, bringing new breakthroughs in the treatment of vascular diseases and providing more possibilities for the development of new vascular stent products.

4. Application of B-CDs in Vascular Stent Coating

How to coat the surface of vascular stent with B-CDs is the key step to developing new B-CDs coatings. However, since there are no practical examples of B-CDs being applied to the coating of vascular stents, several possible methods of preparing B-CDs coatings will be described in the following sections, taking into account the physical/chemical properties of B-CDs. And the excellent potential of applying B-CDs to vascular stent surfaces will be shared, which is summarized in Figure 6.

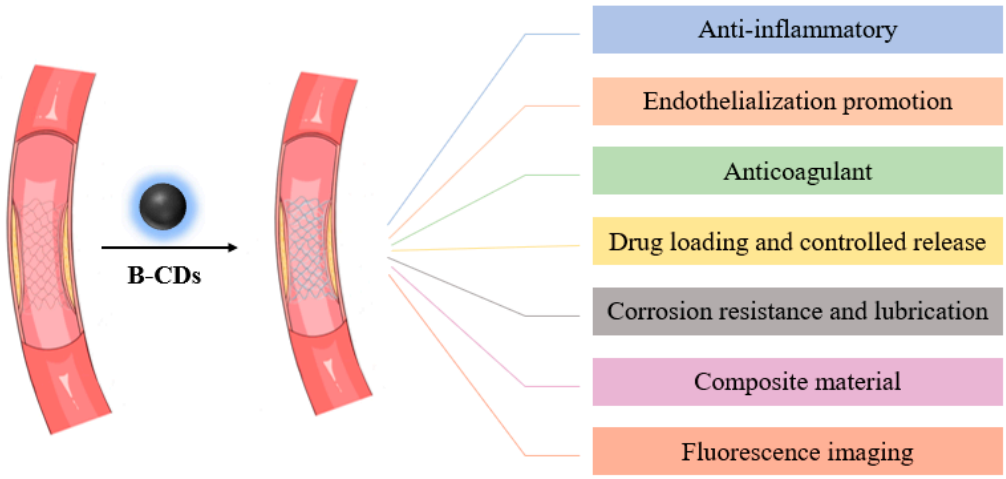

Figure 6. The excellent potential of B-CDs in vascular stent coating.

4.1. Method and Challenges of Coating B-CDs on the Surface of Vascular Stent

B-CDs can be directly coated on the surface of the vascular stent by soaking, spraying, etc. The surface of a vascular scaffold usually has a certain roughness and chemically active site, which provides a physical attachment point for B-CDs adsorption. The high surface energy of B-CDs can also increase the tendency to interact with vascular stents. The abundant hydroxyl, carboxyl, amino, and other functional groups on the surface of B-CDs can interact with metal ions and oxides on the surface of vascular scaffolds, such as forming hydrogen bonds and ionic bonds so that B-CDs can be firmly adsorbed on the surface of vascular scaffolds [126]. In addition, the vascular scaffold surface can also be activated to make it have groups that can react with the functional groups of the B-CDs surface. Through chemical reactions, such as the condensation reaction and amidation reaction, B-CDs were covalently grafted to the surface of the vascular stent to form a stable coating. Zhao et al. [127] reported the preparation of antifouling film grafted with B-CDs. The carboxyl group of B-CDs is aminated with the amine group of

polydopamine, and B-CDs are fixed on the polydopamine film. B-CDs can be directly coated on the surface of the vascular stent by layer self-assembly. The B-CDs surface carries a specific charge, and the B-CDs and other functional molecules are alternately assembled on the surface of the vascular scaffold to form a B-CDs coating with a multi-layer structure. Deng et al. [128] prepared a positive permeable membrane using PEI as a positive layer and B-CDs prepared with milk as a precursor system as a negative layer through the layer self-assembly method. Or by the electrochemical deposition method, a certain voltage or current is applied to the vascular stent in the electrolyte containing B-CDs so that the B-CDs move to the surface of the stent under the action of an electric field and are deposited on the surface so as to achieve the purpose of coating the B-CDs on the surface of the vascular stent. Wang et al. [129] used electrochemical deposition to fix CDs prepared by arc discharge on the outer wall of TiO_2 nanotubes.

Vascular stents have complex geometric shapes, including tubular structures, grids, or pores of the scaffolds. It is a great challenge to achieve a uniform distribution of B-CDs coatings on these irregular surfaces; otherwise, the substrate of the vascular stent will be exposed, reducing the biocompatibility of the vascular stent. Coating thickness is also an important parameter to consider. A too-thick coating may affect the mechanical properties of the stent, and a too-thin coating may not be able to play the functions of B-CDs coating, such as drug slow release, anticoagulation, and other functions that may be greatly reduced. Stents can be used for periods ranging from a few days to several years, and it is important to be able to maintain stability in the complex physiological environment in the body. Under the wash of blood, the coating may dissolve, peel, or change its chemical structure, affecting the therapeutic effect of the stent. Moreover, the surface properties of different stent materials vary greatly, and the way of coating B-CDs needs to be matched with the specific stent materials.

4.2. The Potential of B-CDs as Coating Materials for Vascular Stents

4.2.1. Anti-Inflammatory

After the implantation of vascular stents, the inflammatory mechanism plays a crucial role, affecting the function of the stents and the long-term prognosis of patients. Excessive inflammatory response is one of the important factors leading to restenosis after vascular stent implantation. The inflammations that may be triggered after vascular stent implantation mainly include foreign-body-reactive inflammation and inflammatory responses after local tissue injury. When a vascular stent is implanted, the body regards it as a foreign body and will initiate an immune response. At the same time, the implantation of the stent may cause certain damage to tissues such as the vascular endothelium, resulting in the deposition and activation of platelets. These platelets release inflammatory mediators at the damaged site, attracting more immune cells such as macrophages and lymphocytes to gather around the stent, producing inflammatory mediators and causing an inflammatory response [130]. In addition, the inflammatory response promotes the migration and proliferation of smooth muscle cells towards the intimal area, leading to the formation of neointima. It may also cause vascular remodeling and negative remodeling, thereby increasing the risk of ISR [131,132].

Macrophages (MAs) are distributed in almost every organ in the human body. Studies have shown that the mitochondria of macrophages play a crucial role in inducing chronic inflammation [133]. Reactive oxygen species (ROS) are mainly synthesized by mitochondria, and excessive ROS can induce inflammation [134]. ROS can regulate the synthesis of multiple inflammation markers, and its high reactivity will cause severe damage to cells and even cell apoptosis [135,136]. Yang et al. [137] prepared water-insoluble lutein into B-CDs with good water solubility and biocompatibility by the hydrothermal method and retained their high reducing ability. Non-fluorescent DCFH-DA (ROS fluorescent detection probe) is hydrolyzed into DCFH by cellulase after entering the cell, and then DCFH is converted into fluorescent DCF after combining with intracellular ROS. The research results show that after B-CDs enter the cell through endocytosis, the fluorescence intensity of the cell decreases, indicating that

B-CDs can effectively scavenge intracellular ROS and prevent the combination of DCFH and ROS. This may be due to the redox reaction between the oxygen-containing functional groups (such as hydroxyl groups, carboxyl groups, etc.) on the surface of B-CDs and ROS, thereby converting reactive oxygen species into more stable substances to achieve the scavenging effect. Therefore, the presence of B-CDs can reduce the damage of oxidative stress to cells and further reduce excessive cellular inflammation. Qiang et al. [138] prepared safflower- and Angelica-derived B-CDs by the hydrothermal method. The research results demonstrated that these two types of B-CDs can not only reduce the friction coefficient but also inherit the anti-inflammatory effects of their Chinese medicine precursors. Injection of B-CDs can reduce the expression of pro-inflammatory cytokines (IL-1, IL-6, TNF-α) in the serum of rat models with rheumatoid arthritis. Zhao et al. [139] synthesized a negatively charged B-CD named Vaccaria Semen by pyrolysis, which has good low toxicity and blood compatibility. In this experiment, CCK-8 was used to determine the proliferation effect of RAW264.7 cells under different B-CD concentrations, and the cell survival rate was as high as 195% when the concentration reached 125 μg/mL. B-CDs significantly decreased the levels of TNF-α, IL-6, and IL-1β in the liver tissue of mice with hepatic fibrosis, suggesting that B-CDs inhibited inflammatory response. The application of ROS scavenging ability or anti-inflammatory effect of B-CDs on the surface of vascular stents may reduce the inflammatory response after stent implantation and help to improve the biocompatibility of stent coating with vascular tissue so that the stent can better integrate into the vascular environment.

4.2.2. Endothelialization Promotion

The first contact of B-CDs after entering the blood is the ECs of blood vessels, so it is very important to evaluate the effect of B-CDs on endothelial cells (ECs). Rapid endothelialization in situ after stent implantation is a promising therapeutic method to inhibit local thrombosis and restenosis, which has been paid more and more attention. The effect of B-CDs on ECs may depend on a number of factors, including the size of the B-CDs, surface chemistry, surface functional groups, concentration, and preparation method. Sharma, A et al. [13] used citric acid and urea as precursors to prepare B-CDs by the solvothermic method and evaluated the effects of B-CDs on the proliferation and migration of ECs. As shown in Figure 7a, ECs treated with B-CDs have a significant proliferation phenomenon compared with ECs not treated with B-CDs. As shown in Figure 7b, after B-CDs entered the ECs, most of them were distributed in the cytoplasm. As shown in Figure 7c, compared with ECs treated without B-CDs, the ECs scratch area after B-CDs treatment becomes narrower, indicating that B-CDs can stimulate ECs migration. As shown in Figure 7d, the formation of new vascular networks indicates the formation of blood vessels. Compared with the control group, the branches, ring numbers, and tube lengths of the new vascular networks in cells treated with B-CDs are increased, indicating that B-CDs can promote angiogenesis. Cheng et al. [121] synthesized B-CDs with citric acid and resveratrol, which still proved that B-CDs can promote the proliferation and migration of ECs, and B-CDs can be rapidly taken up by cells within 12 h and well-metabolized by cells after 24 h. In particular, the effect is most significant when the concentration of B-CDs is 200 μg/mL. The rat skin defect model showed that the B-CDs group had a large number of new angiogenesis and rapid wound healing. This again suggests that B-CDs promote the proliferation of endothelial cells in the blood vessel wall and increase the rate of endothelial cell migration, leading to faster vascular healing. The introduction of B-CDs may promote rapid cell division and growth by activating the proliferation signaling pathway of endothelial cells or regulating the cell cycle-related proteins.

B-CDs, which have the ability to clear ROS, also play an important role in its proliferation. Oxidative stress usually inhibits cell growth, while B-CDs can effectively reduce ROS levels under cell culture conditions, thereby protecting cells and promoting their proliferation [140]. B-CDs were also found to inhibit TNF-α-induced endothelial inflammation. This effect is achieved by clearing hydroxides and upregulating the expression of antioxidant genes, thereby improving the living environment of ECs and further promoting their proliferation [141]. In summary, B-CDs show great potential in promoting EC prolif-

eration, but the specific mechanism of regulating EC proliferation and migration remains to be further explored. The design and preparation of specific B-CDs may promote the proliferation, migration, and angiogenesis of ECs by providing suitable surface properties, releasing bioactive molecules, or regulating cell signaling pathways. Therefore, if B-CDs with these properties are applied to the coating of a vascular stent, it may also promote endothelialization and angiogenesis of the stent.

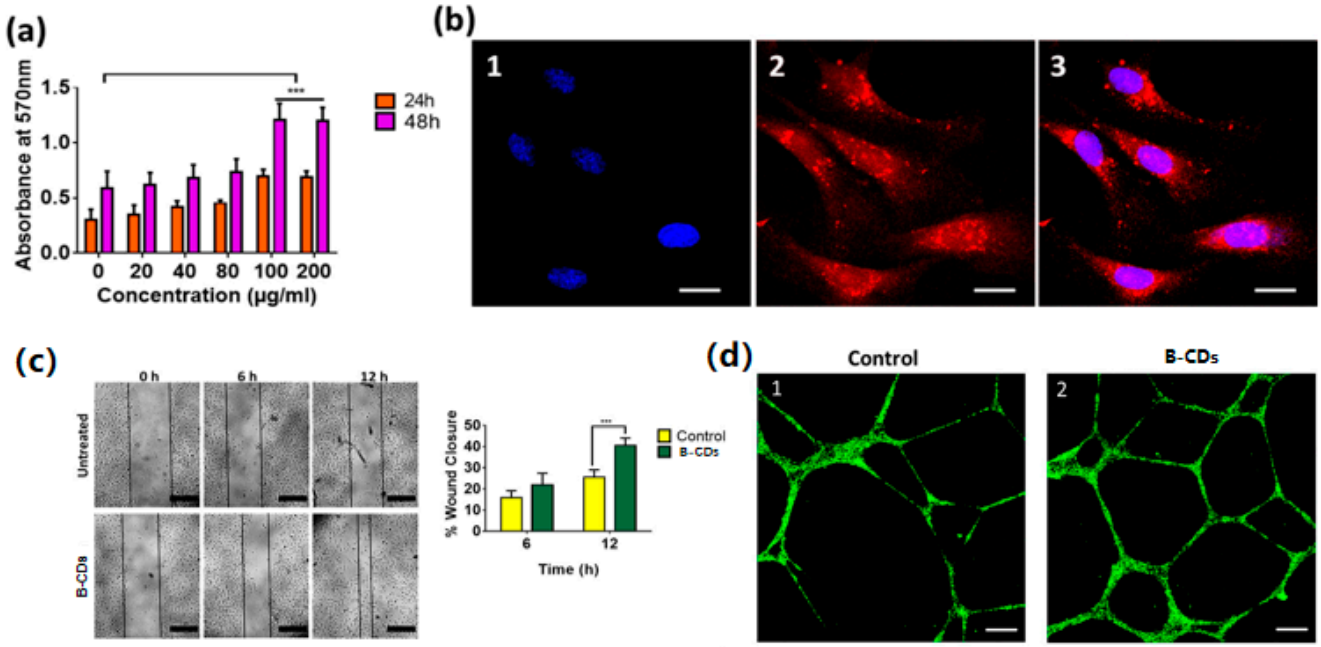

Figure 7. (**a**) MTT assay of HUVEC treated with B-CDs for 24 h and 48 h; (**b**) confocal images of HUVEC incubated with B-CDs (100 µg/mL) for 24 h: (1) cell nucleus stained blue with Hoechst, (2) CDs–urea (red) uptake in the cells, and (3) merged images of parts 1 and 2. The scale bar represents 20 µm; (**c**) migratory response of HUVEC to B-CDs. (**d**) Confocal images of the network formed by untreated control cells and in cells treated with B-CDs (100 µg/mL) for 6 h. (***) p value of $\leq$0.001 (student's t test). The scale bar represents 200 µm [13].

4.2.3. Anticoagulant

Blood coagulation is achieved by the clotting system (clotting factors, fibrinogen, and platelets), and platelet activation and aggregation are key steps in thrombosis. B-CDs prepared by the hydrothermal method of α-cyclodextrin and KH_2PO_4 have anticoagulant properties at high concentrations, which may be the reason for the interaction of B-CDs with coagulation factors or fibrinogen and possibly impair their biological function [142]. B-CDs with specific surface modifications may extend the clotting time and exhibit anticoagulant properties. For example, the introduction of carboxyl groups may increase the electronegativity of B-CDs, and these groups reduce the binding of platelets to B-CDs and inhibit platelet aggregation through electrostatic repulsion, thus achieving an anticoagulant effect. The introduction of amino groups can enhance the positivity of B-CDs, thereby affecting their interaction with cells and proteins in the blood. Positively charged B-CDs may bind to clotting factors or platelets, change the active conformation of clotting factors, or prevent them from participating in the clotting cascade, thus inhibiting the clotting process. Albumin is the most important protein in human plasma, which has the role of maintaining body nutrition and osmotic pressure. Fedel, M et al. [143] demonstrated that carbon-based materials can bind to protein globular molecules and inhibit the adhesion and activation of platelets on the surface of carbon coatings. B-CDs, as a new type of nano-carbon material, may also inhibit platelet adhesion and activation and thus play an anticoagulant effect. The application of B-CDs with anticoagulant properties to the coating of vascular stent can change the properties of the stent surface, which may inhibit

the adhesion and aggregation of platelets, improve the blood compatibility of vascular stent, maintain the normal flow of blood, and reduce the risk of thrombosis after stent implantation.

Ca^{2+} is an essential element in the clotting process. It is involved in almost all the clotting stages except coagulation factor XII, XI, and kinin pathway. It is involved in the activation of thrombin and the conversion of prothrombin to thrombin. Therefore, by reducing the concentration of Ca^{2+} in the blood, it can interfere with the clotting process and play an anticoagulant effect [144]. Yue et al. [145] prepared non-toxic CDs modified based on ethylenebis (oxyethylenenitrilo) tetraacetic acid (EGTA) by a two-step hydrothermal method. First, citric acid and ethylenediamine were hydrothermal prepared in a one-step CDs solution, and after cooling, 1 g additional EGTA was added to the solution for secondary hydrothermal synthesis to achieve the cross-linking of the carboxyl and amino groups of CDs. As shown in Figure 8, a copper ion can coordinate with multiple CDs, and the CDs can be aggregated through complexation. If B-CDs with this characteristic are applied to the surface of the vascular stent, it can reduce the concentration of Ca^{2+} in blood, achieve the purpose of anticoagulation, and then reduce the possibility of thrombosis. In addition, the combination of B-CDs with other anticoagulant drugs may also further enhance its anticoagulant effect. This is particularly important for reducing acute and subacute stent thrombosis events.

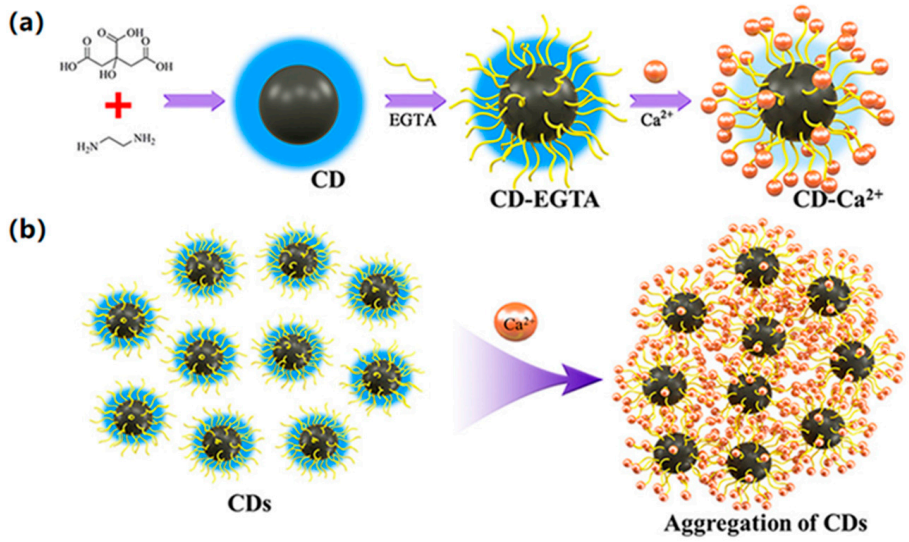

Figure 8. (**a**) Illustration for Ca^{2+} detection by EGTA-modified CDs; (**b**) schematic diagram of CDs aggregation [145].

4.2.4. Drug Loading and Controlled Release

The surface of B-CDs can be chemically modified to introduce different functional groups, such as a carboxyl group, amino group, hydroxyl group, etc. [146]. These functional groups can interact with drug molecules through covalent or non-covalent bonds to achieve drug loading [147]. By modifying the B-CDs surface, the loading and release of different drugs can be realized, and then the combination therapy and targeted drug delivery can be realized, and the therapeutic effect can be improved [23,148]. B-CDs with smaller particle sizes may have a higher specific surface area and can provide more drug-loading sites, and some B-CDs with pore structures can achieve high drug-loading [149]. The release of drug molecules may be controlled by adjusting pH [150], temperature, or light. For example, some BCDs accumulate when exposed to light, resulting in accelerated drug release [151]. This controlled release property allows the drug to be released at a specific time and place, improving the therapeutic effectiveness of the drug while reducing the side effects of the drug. In addition, because B-CDs have good dispersion and stability, they can effectively improve the solubility of hydrophobic drugs and extend their half-life in vivo. This property is particularly suitable for drugs that are difficult to dissolve in water

and can be released slowly in the body, thus reducing the side effects of the drug [149,152]. B-CDs coatings can also combine with drugs to form DES. By controlling the concentration and distribution of B-CDs, the drug release rate can be adjusted so that anti-proliferative drugs can be released continuously after implantation and the incidence of vascular restenosis can be reduced [153,154]. B-CDs with a nanoscale size can easily pass through various barriers in organisms, such as blood vessel walls, cell membranes, and the BBB, etc., thereby achieving efficient drug delivery. The existence of the BBB makes it difficult for many drugs to enter the brain, which brings difficulties to the treatment of cerebrovascular diseases by vascular stents carrying drugs. However, numerous studies have proven that B-CDs and their conjugates can successfully penetrate the BBB [155]. Applying drug-loaded B-CDs to vascular stent coatings can enhance the drug's ability to cross the blood–brain barrier, which provides new ideas for the treatment of cerebrovascular diseases using vascular stents. The synergy between B-CDs and drugs makes it possible to develop multi-functional vascular stents. For example, B-CDs can be combined with drugs that have functions such as anticoagulation, anti-inflammation, and promotion of vascular endothelialization to fabricate vascular stents with multiple therapeutic functions. B-CDs coatings containing drugs or drug carriers can be used to control the rate at which drugs are released in a specific area, providing a more precise therapeutic effect. The fluorescent properties of B-CDs allow them to be used as a probe for bioimaging, helping researchers monitor the process of drug release on the stent and its distribution in the body in real-time. This is important for understanding the drug release mechanism and biological interactions [148,156].

4.2.5. Corrosion Resistance and Lubrication

In the early stages of vascular repair, a BVS needs to provide sufficient radial support to keep the blood vessels open. If the degradation rate is too fast, the BVS will lose its supporting role before the blood vessel is fully repaired, which may cause the blood vessel to narrow again or collapse, affecting the effect of surgery. When the blood vessel is repaired to a certain extent, the BVS completes its supporting task and needs to be timely degraded in order to restore the normal physiological function and elasticity of the blood vessel. Studies have proved that B-CDs also have a good performance in the field of corrosion prevention. B-CDs can form a single molecular layer on the metal surface by electrostatic adsorption. This adsorption mainly depends on the nitrogen and oxygen elements rich in its surface, which are relatively electronegative, so that B-CDs can effectively combine with the metal surface to form a protective film so as to isolate the corrosive medium. This protective film can significantly reduce the corrosion rate of the metal and reduce the damage degree of the metal in a corrosive environment [157,158]. Many studies have proven that B-CDs have great potential in inhibiting the corrosion of carbon steel, copper alloy, magnesium alloy, etc. [159–162]. Darani, MK et al. [163] dispersed B-CDs prepared with citric acid and m-phenylenediamine in aqueous epoxy electrodeposition coatings, and a series of anti-corrosion studies proved that coatings with B-CDs added had better corrosion inhibition and protection of metal matrix. If there are some functional groups (such as nitrogen atoms, etc.) on the surface of B-CDs that can provide lone pairs of electrons, and the magnesium atoms on the surface of magnesium alloys have empty orbitals, then the nitrogen atoms on the surface of B-CDs can provide lone pairs of electrons to the magnesium atoms to form coordination bonds. It has been reported that nitrogen-doped CDs synthesized by the hydrothermal method were added to an electroplating solution to an electroplate nickel-based coating on the surface of magnesium alloy, which significantly improved the wear and corrosion resistance of magnesium alloy [164]. The degradation rate of magnesium alloy biodegradable gold vascular stents is too fast. Grafting it to the surface of the stent may reduce the degradation rate of the stent and prolong the service life of the stent. B-CDs also have unique tribological properties, such as rolling effects and repair effects, which can improve the lubrication properties of metal surfaces. This lubricating layer not only reduces friction but also effectively reduces wear on the surface of the bracket, further enhancing its corrosion resistance. Bilas, P et al. [165] prepared B-CDs with sargasso, and

the average friction coefficient measured by adding it to lubricating oil was 78% lower than that measured by pure water-based lubricating oil. B-CDs prepared from safflower [138], citric acid [166,167], glucose [168], and other biomass materials have been successfully used as lubricants or lubricating oil additives. B-CDs as a new type of environmental protection corrosion-resistant material, through their rich functional groups, excellent lubrication performance, and the ability to form a protective film, significantly improve the properties of the metal surface. These characteristics make B-CDs have broad application prospects in the field of corrosion prevention and vascular stent coating.

4.2.6. Other Potential

Studies have shown that combining B-CDs with other biocompatible materials can improve the self-expanding properties of the scaffold. For example, Duarah, R et al. [169] designed a bio-based hyperbranched polyurethane/silver carbon point (HPU/CD-Ag) nanocomposite and used it to develop a rapid self-expanding scaffold that achieved 20 s rapid self-expansion (>99%) at 37 °C. This indicates that the addition of B-CDs can significantly improve the mechanical properties of the stent. Mahmud, A et al. [170] designed a bioabsorbable polymer scaffold using 3D printing technology based on fuse manufacturing. The composite material of the scaffold was composed of bioabsorbable polylactic acid and B-CDs, wherein B-CDs were prepared by the curcumin hydrothermal method. This may be due to the fact that there are many hydrophilic groups on the surface of B-CDs, and the high surface area to volume ratio of B-CDs makes it form an effective strengthening effect in the microstructure of the scaffold material, thereby improving some mechanical properties of the scaffold. If B-CDs are applied to the coating of vascular scaffolds, it may also increase some mechanical properties of the scaffolds, such as hydrophilicity, wear resistance, and promoting cell proliferation, so as to improve the long-term stability and durability of the scaffolds.

B-CDs coating can act as a physical barrier, reduce the direct contact between the metal scaffold substrate and body fluid, reduce the dissolution of metal ions, and reduce the possible toxic reaction. It can also reduce the friction and stimulation of the blood vessel wall and reduce the irritation and damage to the blood vessels. In addition, the coating can also play a certain physical barrier effect to prevent the stent material from contacting with blood and vascular tissue directly. There are studies using waste coconut shell fiber as a carbon source and using the thermal calcination method to prepare B-CDs. The hemolysis rate of human blood increased linearly with the increase in B-CD concentration, but the overall hemolysis rate was less than 5%, indicating that B-CDs had good blood compatibility [171]. B-CDs themselves are characterized by low toxicity and outstanding biocompatibility, and a large number of experiments have proven that B-CDs composite with other materials can improve the performance of other materials. For example, the binding of CDs to porphyrins not only preserves the pH sensitivity of CDs but also reduces the hemolysis rate of the complex [172]. A novel multi-functional CDs-drug delivery system synthesized by the agitation method AMP-CDs@5-Fu (AMP is a polysaccharide from Allium macrostemon Bunge, 5-Fu is a classic anticancer). The toxicity and hemolysis rate of 5-Fu were significantly reduced, and the anti-tumor ability of 5-Fu was significantly improved [173]. In the future, it is possible to combine B-CDs with other functional materials to design a composite coating doped with B-CDs, which can not only retain the characteristics of B-CDs themselves but also have the functions of other materials and prepare a new type of vascular stent with more functions.

The fluorescent properties of B-CDs enable them to be used as imaging agents, which can be used for real-time tracer diagnosis after vascular stent implantation, helping doctors monitor the position and distribution of the stent and ensuring that the stent is correctly supporting the blood vessel [148]. Specifically, the fluorescence properties of B-CDs can be used to make a contrast agent for fluorescence imaging, through imaging techniques such as fluorescence microscopy or imaging spectrometers, to observe the distribution and interaction of scaffolders in blood vessels in real-time. This real-time tracer capability is of

great significance for optimizing interventional therapy strategies, reducing complications, and improving therapeutic outcomes.

5. Conclusions and Outlook

In this paper, the selection, preparation, and modification of B-CDs as well as the application prospect of B-CDs in the field of vascular stent coating are reviewed in detail. By exploring new biomass sources and improving the preparation process or surface modification, B-CDs can be made to have anti-inflammatory, endothelialization-promoting, anticoagulation, and fluorescence imaging properties, which will play an important role in the application of vascular stents. Although B-CDs show extraordinary potential in the coating of vascular stents, there may be some challenges in practical applications, such as ensuring coating uniformity, long-term stability, and the feasibility of large-scale production. Future research may focus on improving B-CDs synthesis methods, synergies with drugs, optimizing coating processes, and exploring more functionalization strategies to fully realize the potential of B-CDs in vascular stents. At the same time, the long-term biosafety and biodegradability of B-CDs coating in vivo is also one of the future improvement directions. In addition, the study of B-CDs coatings also involves the combination of composites with other materials, such as metals or other nanoparticles, to create scaffolders with additional functions, such as promoting endothelialization or anti-inflammatory properties. The research and development of these composites may overcome the limitations that traditional stent materials may have and provide a more comprehensive treatment solution. In this paper, the application prospects and challenges of B-CDs in vascular stent coating were preliminarily discussed, and further research and practical verification are needed in the future. It is believed that along with the continuous development of science and technology, more innovative applications based on B-CDs are expected to appear in the field of cardiovascular and cerebrovascular stents in the future.

Author Contributions: Conceptualization, J.L. and H.D.; investigation, H.D., Y.W., L.C. and Z.Z.; writing—original draft preparation, H.D.; writing—review and editing, J.L., L.C. and A.A.; supervision, J.L. and L.C.; funding acquisition, J.L. and L.C. All authors have read and agreed to the published version of the manuscript.

Funding: This research was funded by the National Natural Science Foundation of China, grant number 52101292/U2004164; the Key Scientific and Technological Research Projects in Henan Province, grant numbers 232102311155 and 232102230106; the Joint Founds of the R&D Program of Henan Province (No. 222301420055); the Zhengzhou University Major Project Cultivation Special Project, grant number 125-32214076.

Acknowledgments: Figures 1 and 3 reproduced from Ref. [6] with permission from John Wiley and Sons (License Number: 5884280618753); Figure 7 was reprinted (adapted) with permission from {Sharma, A.; Panwar, V.; Chopra, V.; Thomas, J.; Kaushik, S.; Ghosh, D. Interaction of Carbon Dots with Endothelial Cells: Implications for Biomedical Applications. *ACS Applied Nano Materials* **2019**, *2*, 5483–5491}, copyright {2019}, the American Chemical Society; Figure 8 was reprinted (adapted) with permission from {Yue, J.; Li, L.; Cao, L.; Zan, M.; Yang, D.; Wang, Z.; Chang, Z.; Mei, Q.; Miao, P.; Dong, W.-F. Two-Step Hydrothermal Preparation of Carbon Dots for Calcium Ion Detection. *ACS Applied Materials & Interfaces* **2019**, *11*, 44566–44572}, copyright {2019}, the American Chemical Society.

Conflicts of Interest: The authors declare no conflicts of interest.

Abbreviations

B-CDs	Biomass-derived carbon dots
BBB	Blood–brain barrier
BMS	Bare metal stent
BVS	Biodegradable vascular stent
CDs	Carbon dots
DMF	Dimethylformamide
DESs	Drug-eluting stents

ECs	Endothelial cells
MA	Macrophage
ISR	In-stent restenosis
PEI	Polyethyleneimine
PEG	Polyethylene glycol
PCI	Percutaneous coronary intervention
QY	Quantum yield
ROS	Reactive oxygen species
TCMs	Traditional Chinese medicines

References

1. National Center For Cardiovascular Diseases The Writing Committee Of The Report On Cardiovascular Health And Diseases In China. Report on Cardiovascular Health and Diseases in China 2023: An Updated Summary. *Biomed. Environ. Sci. BES* **2024**, *37*, 949–992.
2. Hou, Y.; Zhang, X.; Li, J.; Wang, L.; Guan, S. A multi-functional MgF_2 /polydopamine/hyaluronan-astaxanthin coating on the biodegradable ZE21B alloy with better corrosion resistance and biocompatibility for cardiovascular application. *J. Magnes. Alloys* **2024**, *12*, 1102–1116. [CrossRef]
3. Buccheri, D.; Piraino, D.; Andolina, G.; Cortese, B. Understanding and managing in-stent restenosis: A review of clinical data, from pathogenesis to treatment. *J. Thorac. Dis.* **2016**, *8*, E1150–E1162. [CrossRef] [PubMed]
4. Xu, X.Y.; Ray, R.; Gu, Y.L.; Ploehn, H.J.; Gearheart, L.; Raker, K.; Scrivens, W.A. Electrophoretic analysis and purification of fluorescent single-walled carbon nanotube fragments. *J. Am. Chem. Soc.* **2004**, *126*, 12736–12737. [CrossRef]
5. Sun, Y.-P.; Zhou, B.; Lin, Y.; Wang, W.; Fernando, K.A.S.; Pathak, P.; Meziani, M.J.; Harruff, B.A.; Wang, X.; Wang, H.; et al. Quantum-sized carbon dots for bright and colorful photoluminescence. *J. Am. Chem. Soc.* **2006**, *128*, 7756–7757. [CrossRef]
6. Ai, L.; Shi, R.; Yang, J.; Zhang, K.; Zhang, T.; Lu, S. Efficient Combination of G-C_3N_4 and CDs for Enhanced Photocatalytic Performance: A Review of Synthesis, Strategies, and Applications. *Small* **2021**, *17*, 2007523. [CrossRef]
7. Ghasemi, Y.; Peymani, P.; Afifi, S. Quantum dot: Magic nanoparticle for imaging, detection and targeting. *Acta Bio-Medica Atenei Parm.* **2009**, *80*, 156–165.
8. Basu, A.; Suryawanshi, A.; Kumawat, B.; Dandia, A.; Guin, D.; Ogale, S.B. Starch (Tapioca) to carbon dots: An efficient green approach to an on-off-on photoluminescence probe for fluoride ion sensing. *Analyst* **2015**, *140*, 1837–1841. [CrossRef]
9. Gao, W.; Song, H.; Wang, X.; Liu, X.; Pang, X.; Zhou, Y.; Gao, B.; Peng, X. Carbon Dots with Red Emission for Sensing of Pt^{2+}, Au^{3+}, and Pd^{2+} and Their Bioapplications in Vitro and in Vivo. *Acs Appl. Mater. Interfaces* **2018**, *10*, 1147–1154. [CrossRef]
10. Li, D.; Jing, P.; Sun, L.; An, Y.; Shan, X.; Lu, X.; Zhou, D.; Han, D.; Shen, D.; Zhai, Y.; et al. Near-Infrared Excitation/Emission and Multiphoton-Induced Fluorescence of Carbon Dots. *Adv. Mater.* **2018**, *30*, 1705913. [CrossRef]
11. Wang, B.; Cai, H.; Waterhouse, G.I.N.; Qu, X.; Yang, B.; Lu, S. Carbon Dots in Bioimaging, Biosensing and Therapeutics: A Comprehensive Review. *Small Sci.* **2022**, *2*, 2200012. [CrossRef]
12. Geng, B.; Li, P.; Fang, F.; Shi, W.; Glowacki, J.; Pan, D.; Shen, L. Antibacterial and osteogenic carbon quantum dots for regeneration of bone defects infected with multidrug-resistant bacteria. *Carbon* **2021**, *184*, 375–385. [CrossRef]
13. Sharma, A.; Panwar, V.; Chopra, V.; Thomas, J.; Kaushik, S.; Ghosh, D. Interaction of Carbon Dots with Endothelial Cells: Implications for Biomedical Applications. *Acs Appl. Nano Mater.* **2019**, *2*, 5483–5491. [CrossRef]
14. Shaik, S.A.; Sengupta, S.; Varma, R.S.; Gawande, M.B.; Goswami, A. Syntheses of N-Doped Carbon Quantum Dots (NCQDs) from Bioderived Precursors: A Timely Update. *Acs Sustain. Chem. Eng.* **2021**, *9*, 3–49. [CrossRef]
15. Xu, Y.; Wang, C.; Zhuo, H.; Zhou, D.; Song, Q. The function-oriented precursor selection for the preparation of carbon dots. *Nano Res.* **2023**, *16*, 11221–11249. [CrossRef]
16. Li, Y.; Gao, J.; Shi, Y.; Wang, Y.; Li, M.; Pan, A.; Hu, M.; Zhang, G. Insight into the synthesis of carbon quantum dots by gas-liquid discharges: The role of precursors. *Carbon* **2024**, *218*, 118653. [CrossRef]
17. Nguyen, K.G.; Hus, M.; Baragau, I.-A.; Bowen, J.; Heil, T.; Nicolaev, A.; Abramiuc, L.E.; Sapelkin, A.; Sajjad, M.T.; Kellici, S. Engineering Nitrogen-Doped Carbon Quantum Dots: Tailoring Optical and Chemical Properties through Selection of Nitrogen Precursors. *Small* **2024**, *20*, 2310587. [CrossRef]
18. Sun, R.; Liu, S. Synthesis of photoluminescent carbon dots and its effect on chondrocytes for knee joint therapy applications. *Artif. Cells Nanomed. Biotechnol.* **2019**, *47*, 1321–1325. [CrossRef]
19. Sun, H.; Yang, G.; Yang, B. Synthesis, Structure Control and Applications of Carbon Dots. *Chem. J. Chin. Univ. -Chin.* **2021**, *42*, 349–365.
20. Wang, H.-J.; Yu, T.-T.; Chen, H.-L.; Nan, W.-B.; Xie, L.-Q.; Zhang, Q.-Q. A self-quenching-resistant carbon dots powder with tunable solid-state fluorescence and their applications in light-emitting diodes and fingerprints detection. *Dye. Pigment.* **2018**, *159*, 245–251. [CrossRef]
21. Siddique, A.B.; Pramanick, A.K.; Chatterjee, S.; Ray, M. Amorphous Carbon Dots and their Remarkable Ability to Detect 2,4,6-Trinitrophenol. *Sci. Rep.* **2018**, *8*, 9770. [CrossRef] [PubMed]

22. Kang, C.; Huang, Y.; Yang, H.; Yan, X.F.; Chen, Z.P. A Review of Carbon Dots Produced from Biomass Wastes. *Nanomaterials* **2020**, *10*, 2316. [CrossRef] [PubMed]
23. Meng, W.; Bai, X.; Wang, B.; Liu, Z.; Lu, S.; Yang, B. Biomass-Derived Carbon Dots and Their Applications. *Energy Environ. Mater.* **2019**, *2*, 172–192. [CrossRef]
24. Oluyinka, O.A.; Oke, E.A.; Oyelude, E.O.; Abugri, J.; Raheem, S.A. Recapitulating potential environmental and industrial applications of biomass wastes. *J. Mater. Cycles Waste Manag.* **2022**, *24*, 2089–2107. [CrossRef]
25. Ragazzon, G.; Cadranel, A.; Ushakova, E.V.; Wang, Y.; Guldi, D.M.; Rogach, A.L.; Kotov, N.A.; Prato, M. Optical processes in carbon nanocolloids. *Chem* **2021**, *7*, 606–628. [CrossRef]
26. Ge, G.; Li, L.; Chen, M.; Wu, X.; Yang, Y.; Wang, D.; Zuo, S.; Zeng, Z.; Xiong, W.; Guo, C. Green Synthesis of Nitrogen-Doped Carbon Dots from Fresh Tea Leaves for Selective Fe^{3+} Ions Detection and Cellular Imaging. *Nanomaterials* **2022**, *12*, 986. [CrossRef]
27. Isnaeni; Rahmawati, I.; Intan, R.; Zakaria, M. Photoluminescence study of carbon dots from ginger and galangal herbs using microwave technique. In Proceedings of the 3rd International Symposium on Frontier of Applied Physics (ISFAP) Part of Indonesian Science Expo, Jakarta, Indonesia, 23–24 October 2017.
28. Algarra, M.; dos Orfaos, L.; Alyes, C.S.; Moreno-Tost, R.; Soledad Pino-Gonzalez, M.; Jimenez-Jimenez, J.; Rodriguez-Castellon, E.; Eliche-Quesada, D.; Castro, E.; Luque, R. Sustainable Production of Carbon Nanoparticles from Olive Pit Biomass: Understanding Proton Transfer in the Excited State on Carbon Dots. *ACS Sustain. Chem. Eng.* **2019**, *7*, 10493–10500. [CrossRef]
29. Huang, Q.; Wu, C.; Teng, Y.; Yang, Y.; Liang, Y.; Yang, S.; Wang, Z.; Peng, D.; Wang, L.; Chen, W. Research progress of carbon dots derived from traditional Chinese medicine. *Chin. Tradit. Herb. Drugs* **2021**, *52*, 5089–5097.
30. Zhang, J.; Zou, L.; Li, Q.; Wu, H.; Sun, Z.; Xu, X.; Shi, L.; Sun, Z.; Ma, G. Carbon Dots Derived from Traditional Chinese Medicines with Bioactivities: A Rising Star in Clinical Treatment. *Acs Appl. Bio Mater.* **2023**, *6*, 3984–4001. [CrossRef]
31. Li, D.; Xu, K.-y.; Zhao, W.-p.; Liu, M.-f.; Feng, R.; Li, D.-q.; Bai, J.; Du, W.-l. Chinese Medicinal Herb-Derived Carbon Dots for Common Diseases: Efficacies and Potential Mechanisms. *Front. Pharmacol.* **2022**, *13*, 815479. [CrossRef]
32. Han, B.; Shen, L.; Xie, H.; Huang, Q.; Zhao, D.; Huang, X.; Chen, X.; Li, J. Synthesis of Carbon Dots with Hemostatic Effects Using Traditional Chinese Medicine as a Biomass Carbon Source. *Acs Omega* **2023**, *8*, 3176–3183. [CrossRef] [PubMed]
33. Li, J.; Jiang, F.; Chi, Z.; Han, D.; Yu, L.; Liu, C. Development of Enteromorpha prolifera polysaccharide-based nanoparticles for delivery of curcumin to cancer cells. *Int. J. Biol. Macromol.* **2018**, *112*, 413–421. [CrossRef] [PubMed]
34. Vibhute, A.; Patil, T.; Malavekar, D.; Patil, S.; Lee, S.; Tiwari, A.P. Green Synthesis of Fluorescent Carbon Dots from Annona squamosam Leaves: Optical and Structural Properties with Bactericidal, Anti-inflammatory, Anti-angiogenesis Applications. *J. Fluoresc.* **2023**, *33*, 1619–1629. [CrossRef]
35. Luo, W.; Zhang, L.; Li, X.; Zheng, J.; Chen, Q.; Yang, Z.; Cheng, M.; Chen, Y.; Wu, Y.; Zhang, W.; et al. Green functional carbon dots derived from herbal medicine ameliorate blood-brain barrier permeability following traumatic brain injury. *Nano Res.* **2022**, *15*, 9274–9285. [CrossRef]
36. Bhattacharya, T.; Do, H.A.; Rhim, J.-W.; Shin, G.H.; Kim, J.T. Facile Synthesis of Multifunctional Carbon Dots from Spent Gromwell Roots and Their Application as Coating Agents. *Foods* **2023**, *12*, 2165. [CrossRef] [PubMed]
37. Perikala, M.; Bhardwaj, A. Highly Stable White-Light-Emitting Carbon Dot Synthesis Using a Non-coordinating Solvent. *Acs Omega* **2019**, *4*, 21223–21229. [CrossRef]
38. Biazar, N.; Poursalehi, R.; Delavari, H. Optical and Structural Properties of Carbon Dots/TiO_2 Nanostructures Prepared Via DC Arc Discharge in Liquid. In Proceedings of the 6th International Biennial Conference on UltraFine Grained and NanoStructured Materials (UFGNSM), Kish Island, Iran, 12–13 November 2017.
39. Kaczmarek, A.; Hoffman, J.; Morgiel, J.; Moscicki, T.; Stobinski, L.; Szymanski, Z.; Malolepszy, A. Luminescent Carbon Dots Synthesized by the Laser Ablation of Graphite in Polyethylenimine and Ethylenediamine. *Materials* **2021**, *14*, 729. [CrossRef]
40. Isnaeni; Hanna, M.Y.; Pambudi, A.A.; Murdaka, F.H. Influence of Ablation Wavelength and Time on Optical Properties of Laser Ablated Carbon Dots. In Proceedings of the 6th International Conference on Theoretical and Applied Physics (ICTAP), Hasanuddin Univ, Makassar, Indonesia, 19–21 September 2016.
41. Saraswat, S.K.; Mustafa, M.A.; Ghadir, G.K.; Kaur, M.; Lozada, D.F.G.; Alubiady, M.H.s.; Al-Ani, A.M.; Alshahrani, M.Y.; Abid, M.K.; Jumaa, S.S.; et al. Carbon quantum dots: A comprehensive review of green Synthesis, characterization and investigation their applications in bioimaging. *Inorg. Chem. Commun.* **2024**, *162*, 112279. [CrossRef]
42. Xu, Y.; Liu, J.; Zhang, J.; Zong, X.; Jia, X.; Li, D.; Wang, E. Chip-based generation of carbon nanodots via electrochemical oxidation of screen printed carbon electrodes and the applications for efficient cell imaging and electrochemiluminescence enhancement. *Nanoscale* **2015**, *7*, 9421–9426. [CrossRef]
43. Li, R.-l.; Zhao, Z.-b.; Leng, C.-y.; Li, Y.; Ai, L.-s.; Sun, Y.; Wang, X.-z.; Qiu, J.-s. Preparation of carbon dots from carbonized corncobs by electrochemical oxidation and their application in Nabatteries. *New Carbon Mater.* **2023**, *38*, 347–355. [CrossRef]
44. Zheng, X.; Qin, K.; He, L.; Ding, Y.; Luo, Q.; Zhang, C.; Cui, X.; Tan, Y.; Li, L.; Wei, Y. Novel fluorescent nitrogen-doped carbon dots derived from *Panax notoginseng* for bioimaging and high selectivity detection of Cr^{6+}. *Analyst* **2021**, *146*, 911–919. [CrossRef] [PubMed]
45. Alanazi, A.Z.; Alhazzani, K.; Mostafa, A.M.; Barker, J.; El-Wekil, M.M.; Ali, A.-M.B.H. Highly selective fluorometric detection of streptokinase via fibrinolytic release of photoluminescent carbon dots integrated into fibrin clot network. *Microchem. J.* **2024**, *197*, 109800. [CrossRef]

46. Liu, J.; Kong, T.; Xiong, H.-M. Mulberry-Leaves-Derived Red-Emissive Carbon Dots for Feeding Silkworms to Produce Brightly Fluorescent Silk. *Adv. Mater.* **2022**, *34*, 2200152. [CrossRef]
47. Chen, M.; Liu, C.; An, Y.; Li, Y.; Zheng, Y.; Tian, H.; Shi, R.; He, X.; Lin, X. Red, green, and blue light-emitting carbon dots prepared from gallic acid for white light-emitting diode applications. *Nanoscale Adv.* **2021**, *4*, 14–18. [CrossRef]
48. Liu, Y.; Xiao, N.; Gong, N.; Wang, H.; Shi, X.; Gu, W.; Ye, L. One-step microwave-assisted polyol synthesis of green luminescent carbon dots as optical nanoprobes. *Carbon* **2014**, *68*, 258–264. [CrossRef]
49. Tabaraki, R.; Abdi, O. Fluorescent sensing of Pb^{2+} by microwave-assisted synthesized N-doped carbon dots: Application of response surface methodology and Doehlert design. *J. Iran. Chem. Soc.* **2020**, *17*, 839–846. [CrossRef]
50. Liu, Y.; Guo, D.; Gao, Y.; Tong, B.; Li, Y.; Zhu, Y. Non-thermal effect of microwave on the chemical structure and luminescence properties of biomass-derived carbon dots via hydrothermal method. *Appl. Surf. Sci.* **2021**, *552*, 149503. [CrossRef]
51. Chen, B.; Li, F.; Li, S.; Weng, W.; Guo, H.; Guo, T.; Zhang, X.; Chen, Y.; Huang, T.; Hong, X.; et al. Large scale synthesis of photoluminescent carbon nanodots and their application for bioimaging. *Nanoscale* **2013**, *5*, 1967–1971. [CrossRef]
52. Li, S.; Zhao, X.; Zhang, Y.; Chen, H.; Liu, Y. Fluorescent N-doped Carbon Dots from Bacterial Cellulose for Highly Sensitive Bacterial Detection. *Bioresources* **2020**, *15*, 78–88. [CrossRef]
53. Meiyazhagan, A.; Aliyan, A.; Ayyapan, A.; Moreno-Gonzalez, I.; Susarla, S.; Yazdi, S.; Cuanalo-Contreras, K.; Khabashesku, V.N.; Vajtai, R.; Marti, A.A.; et al. Soft-Lithographic Patterning of Luminescent Carbon Nanodots Derived from Collagen Waste. *Acs Appl. Mater. Interfaces* **2018**, *10*, 36275–36283. [CrossRef] [PubMed]
54. Woo, J.; Song, Y.; Ahn, J.; Kim, H. Green one-pot preparation of carbon dots (CD)-embedded cellulose transparent film for Fe^{3+} indicator using ionic liquid. *Cellulose* **2020**, *27*, 4609–4621. [CrossRef]
55. de Oliveira, B.P.; Bessa, N.U.d.C.; do Nascimento, J.F.; Cavalcante, C.S.d.P.; Fontenelle, R.O.d.S.; Abreu, F.O.M.d.S. Synthesis of luminescent chitosan-based carbon dots for Candida albicans bioimaging. *Int. J. Biol. Macromol.* **2023**, *227*, 805–814. [CrossRef] [PubMed]
56. Aung, Y.-Y.; Wibrianto, A.; Sianturi, J.S.; Ulfa, D.K.; Sakti, S.C.W.; Irzaman, I.; Yuliarto, B.; Chang, J.-y.; Kwee, Y.; Fahmi, M.Z. Comparison Direct Synthesis of Hyaluronic Acid-Based Carbon Nanodots as Dual Active Targeting and Imaging of HeLa Cancer Cells. *Acs Omega* **2021**, *6*, 13300–13309. [CrossRef] [PubMed]
57. Inayat, A.; Albalawi, K.; Rehman, A.-u.; Adnan; Saad, A.Y.; Saleh, E.A.M.; Alamri, M.A.; El-Zahhar, A.A.; Haider, A.; Abbas, S.M. Tunable synthesis of carbon quantum dots from the biomass of spent tea leaves as supercapacitor electrode. *Mater. Today Commun.* **2023**, *34*, 105479. [CrossRef]
58. Liu, S.; Cui, H.; Huang, J.; Tian, B.; Bao, J. Osmanthus-derived carbon dots for cell imaging and NIR photothermal therapy. *Mater. Lett.* **2024**, *377*, 137347. [CrossRef]
59. Darwish, H.W.; Mothana, R.A.; Ganguly, S. Pivalic acid based N-doped carbon dots for drug delivery and antioxidant behaviour. *Colloids Surf. A-Physicochem. Eng. Asp.* **2024**, *688*, 133595. [CrossRef]
60. Gencer, O.; Ceven, O.F.; Unlu, C. Triggering excitation independent fluorescence in zinc(II) incorporated carbon dots: Surface passivation of carbon dots with zinc(II) ions by microwave assisted synthesis methods. *Diam. Relat. Mater.* **2022**, *123*, 108874. [CrossRef]
61. Hui, K.C.; Ang, W.L.; Yahya, W.Z.N.; Sambudi, N.S. Effects of nitrogen/bismuth-doping on the photocatalyst composite of carbon dots/titanium dioxide nanoparticles (CDs/TNP) for enhanced visible light-driven removal of diclofenac. *Chemosphere* **2022**, *290*, 133377. [CrossRef]
62. Torrisi, L.; Silipigni, L.; Torrisi, A.; Cutroneo, M. Luminescence in laser-generated functionalized carbon dots. *Opt. Laser Technol.* **2024**, *177*, 111089. [CrossRef]
63. Javeria, H.; Abbas, M.Q.; Chen, S.-H.; Du, Z.-x. Peanut shell carbon quantum dots modified with citric acid: Amplifying visual detection of fluorescence sensitivity for Cu^{2+}. *J. Mater. Chem. A* **2024**, *12*, 16098–16107. [CrossRef]
64. Zhang, L.; Cai, Z.; Liu, Y.; Fan, Y.; She, Y. Fluorescent enhanced endogenous carbon dots derived from green tea residue for multiplex detection of heavy metal ions in food. *Front. Sustain. Food Syst.* **2024**, *8*, 1431792. [CrossRef]
65. Kumar, A.; Kumar, I.; Gathania, A.K.K. Synthesis, characterization and potential sensing application of carbon dots synthesized via the hydrothermal treatment of cow milk. *Sci. Rep.* **2022**, *12*, 22495. [CrossRef] [PubMed]
66. Zhang, L.; Li, B.; Zhou, Y.; Wu, Y.; Sun, Q.; Le, T. Preparation of phosphorus-doped cow milk-derived carbon quantum dots and detection of Au^{3+}. *J. Food Process Eng.* **2023**, *46*, e14349. [CrossRef]
67. Hu, X.; Li, Y.; Xu, Y.; Gan, Z.; Zou, X.; Shi, J.; Huang, X.; Li, Z.; Li, Y. Green one-step synthesis of carbon quantum dots from orange peel for fluorescent detection of Escherichia coli in milk. *Food Chem.* **2021**, *339*, 127775. [CrossRef]
68. Alarfaj, N.A.; El-Tohamy, M.F.; Oraby, H.F. New Immunosensing-Fluorescence Detection of Tumor Marker Cytokeratin-19 Fragment (CYFRA 21-1) Via Carbon Quantum Dots/Zinc Oxide Nanocomposite. *Nanoscale Res. Lett.* **2020**, *15*, 12. [CrossRef]
69. Zhang, H.; Zhou, Q.; Han, X.; Li, M.; Yuan, J.; Wei, R.; Zhang, X.; Wu, M.; Zhao, W. Nitrogen-doped carbon dots derived from hawthorn for the rapid determination of chlortetracycline in pork samples. *Spectrochim. Acta Part A-Mol. Biomol. Spectrosc.* **2021**, *255*, 119736. [CrossRef]
70. Praseetha, P.K.; Litany, R.I.J.; Alharbi, H.M.; Khojah, A.A.; Akash, S.; Bourhia, M.; Mengistie, A.A.; Shazly, G.A. Green synthesis of highly fluorescent carbon quantum dots from almond resin for advanced theranostics in biomedical applications. *Sci. Rep.* **2024**, *14*, 24435. [CrossRef]

71. Naziba, T.A.; Kumar, D.P.; Karthikeyan, S.; Sriramajayam, S.; Djanaguiraman, M.; Sundaram, S.; Ghamari, M.; Rao, R.P.; Ramakrishna, S.; Ramesh, D. Biomass Derived Biofluorescent Carbon Dots for Energy Applications: Current Progress and Prospects. *Chem. Rec.* **2024**, *24*, e202400030. [CrossRef]
72. Singh, V.; Rawat, K.S.; Mishra, S.; Baghel, T.; Fatima, S.; John, A.A.; Kalleti, N.; Singh, D.; Nazir, A.; Rath, S.K.; et al. Biocompatible fluorescent carbon quantum dots prepared from beetroot extract for in vivo live imaging in C-elegans and BALB/c mice. *J. Mater. Chem. B* **2018**, *6*, 3366–3371. [CrossRef]
73. Lou, Y.; Hao, X.; Liao, L.; Zhang, K.; Chen, S.; Li, Z.; Ou, J.; Qin, A.; Li, Z. Recent advances of biomass carbon dots on syntheses, characterization, luminescence mechanism, and sensing applications. *Nano Sel.* **2021**, *2*, 1117–1145. [CrossRef]
74. Zhou, J.; Ge, M.; Han, Y.; Ni, J.; Huang, X.; Han, S.; Peng, Z.; Li, Y.; Li, S. Preparation of Biomass-Based Carbon Dots with Aggregation Luminescence Enhancement from Hydrogenated Rosin for Biological Imaging and Detection of Fe^{3+}. *Acs Omega* **2020**, *5*, 11842–11848. [CrossRef] [PubMed]
75. Zhao, Z.; Shen, Y.; Liu, Y.; Wang, J.; Ma, M.; Pan, J.; Wang, D.; Wang, C.; Li, J. Investigation of silicon doped carbon dots/Carboxymethyl cellulose gel platform with tunable afterglow and dynamic multistage anticounterfeiting. *J. Colloid Interface Sci.* **2024**, *672*, 142–151. [CrossRef] [PubMed]
76. Lu, D.; Tao, R.; Wang, Z. Carbon-based materials for photodynamic therapy: A mini-review. *Front. Chem. Sci. Eng.* **2019**, *13*, 310–323. [CrossRef]
77. Sengupta, J.; Hussain, C.M. Carbon nanomaterials to combat virus: A perspective in view of COVID-19. *Carbon Trends* **2021**, *2*, 100019. [CrossRef]
78. Yanez-Sedeno, P.; Gonzalez-Cortes, A.; Agui, L.; Pingarron, J.M. Uncommon Carbon Nanostructures for the Preparation of Electrochemical Immunosensors. *Electroanalysis* **2016**, *28*, 1679–1691. [CrossRef]
79. Ge, G.; Li, L.; Wang, D.; Chen, M.; Zeng, Z.; Xiong, W.; Wu, X.; Guo, C. Carbon dots: Synthesis, properties and biomedical applications. *J. Mater. Chem. B* **2021**, *9*, 6553–6575. [CrossRef]
80. Liu, Y.; Yong, C.; Tong, B.; Li, Y.; Wang, N.; Lei, Y. Modification of carbon dots derived from biomass by exogenous nitrogen doping: Action mechanism and difference analysis. *Opt. Mater.* **2022**, *134*, 113144. [CrossRef]
81. Tao, Y.; Lin, J.; Wang, D.; Wang, Y. Na^{+}-functionalized carbon dots with aggregation-induced and enhanced cyan emission. *J. Colloid Interface Sci.* **2021**, *588*, 469–475. [CrossRef]
82. Hola, K.; Sudolska, M.; Kalytchuk, S.; Nachtigallova, D.; Rogach, A.L.; Otyepka, M.; Zboril, R. Graphitic Nitrogen Triggers Red Fluorescence in Carbon Dots. *Acs Nano* **2017**, *11*, 12402–12410. [CrossRef]
83. Olla, C.; Cappai, A.; Porcu, S.; Stagi, L.; Fantauzzi, M.; Casula, M.F.; Mocci, F.; Corpino, R.; Chiriu, D.; Ricci, P.C.; et al. Exploring the Impact of Nitrogen Doping on the Optical Properties of Carbon Dots Synthesized from Citric Acid. *Nanomaterials* **2023**, *13*, 1344. [CrossRef] [PubMed]
84. Oh, G.-H.; Kim, B.-S.; Song, Y.; Kim, S. Acid treatment to tune the optical properties of carbon quantum dots. *Appl. Surf. Sci.* **2022**, *605*, 154690. [CrossRef]
85. Molaei, M.J. The optical properties and solar energy conversion applications of carbon quantum dots: A review. *Sol. Energy* **2020**, *196*, 549–566. [CrossRef]
86. Munusamy, S.; Mandlimath, T.R.; Swetha, P.; Al-Sehemi, A.G.; Pannipara, M.; Koppala, S.; Shanmugam, P.; Boonyuen, S.; Pothu, R.; Boddula, R. Nitrogen-doped carbon dots: Recent developments in its fluorescent sensor applications. *Environ. Res.* **2023**, *231*, 116046. [CrossRef] [PubMed]
87. Liu, Y.; Roy, S.; Sarkar, S.; Xu, J.; Zhao, Y.; Zhang, J. A review of carbon dots and their composite materials for electrochemical energy technologies. *Carbon Energy* **2021**, *3*, 795–826. [CrossRef]
88. Nguyen, K.G.; Baragau, I.-A.; Gromicova, R.; Nicolaev, A.; Thomson, S.A.J.; Rennie, A.; Power, N.P.; Tariq Sajjad, M.; Kellici, S. Investigating the effect of N-doping on carbon quantum dots structure, optical properties and metal ion screening. *Sci. Rep.* **2022**, *12*, 13806. [CrossRef]
89. Azami, M.; Wei, J.; Valizadehderakhshan, M.; Jayapalan, A.; Ayodele, O.O.; Nowlin, K. Effect of Doping Heteroatoms on the Optical Behaviors and Radical Scavenging Properties of Carbon Nanodots. *J. Phys. Chem. C* **2023**, *127*, 7360–7370. [CrossRef]
90. He, Q.; Li, Y.; Wang, D.; Xie, J. Facile synthesis of a novel P-doped carbon coated nickel phosphides nanorods as sodium storage anode materials. *J. Mater.* **2024**, *10*, 408–415. [CrossRef]
91. Yu, F.; Ma, M.; Wu, X.; Li, Z.; Bi, H. Synthesis and bioimaging application of red-emissive carbon dots. *Mendeleev Commun.* **2023**, *33*, 343–345. [CrossRef]
92. Hussain, A.; Alajmi, M.F.; Ganguly, S. Pentetic acid derived dual purpose fluorescent carbon dots for pH responsive drug delivery and antioxidant proficiency. *Diam. Relat. Mater.* **2024**, *145*, 111101. [CrossRef]
93. de Souza, O.P.L.; Tiba, D.Y.; Ferreira, J.H.A.; Lieb, L.C.; Canevari, T.C. Non-enzymatic biosensor based on F,S-doped carbon dots/copper nanoarchitecture applied in the simultaneous electrochemical determination of NADH, dopamine, and uric acid in plasma. *Analyst* **2024**, *149*, 2728–2737. [CrossRef]
94. Shi, J.; Zhou, Y.; Ning, J.; Hu, G.; Zhang, Q.; Hou, Y.; Zhou, Y. Prepared carbon dots from wheat straw for detection of Cu^{2+} in cells and zebrafish and room temperature phosphorescent anti-counterfeiting. *Spectrochim. Acta Part A-Mol. Biomol. Spectrosc.* **2022**, *281*, 121597. [CrossRef] [PubMed]
95. Yan, F.; Jiang, Y.; Sun, X.; Bai, Z.; Zhang, Y.; Zhou, X. Surface modification and chemical functionalization of carbon dots: A review. *Microchim. Acta* **2018**, *185*, 424. [CrossRef] [PubMed]

96. Zhu, B.; Sun, S.; Wang, Y.; Deng, S.; Qian, G.; Wang, M.; Hu, A. Preparation of carbon nanodots from single chain polymeric nanoparticles and theoretical investigation of the photoluminescence mechanism. *J. Mater. Chem. C* **2013**, *1*, 580–586. [CrossRef]
97. Sangjan, A.; Boonsith, S.; Sansanaphongpricha, K.; Thinbanmai, T.; Ratchahat, S.; Laosiripojana, N.; Wu, K.C.W.; Shin, H.S.; Sakdaronnarong, C. Facile preparation of aqueous-soluble fluorescent polyethylene glycol functionalized carbon dots from palm waste by one-pot hydrothermal carbonization for colon cancer nanotheranostics. *Sci. Rep.* **2022**, *12*, 10550. [CrossRef]
98. Toutouzas, K.; Stankovic, G.; Takagi, T.; Spanos, V.; Di Mario, C.; Albiero, F.; Corvaja, N.; Chieffo, A.; Sivieri, G.; Colombo, A. Impact of stent length on restenosis rate in small vessels. *J. Am. Coll. Cardiol.* **2002**, *39*, 53A. [CrossRef]
99. He, M.; Dong, J.; Wen, J.; Zhang, Y.; Han, S.Y.; Wang, C.; Gongol, B.; Wei, T.-Y.W.; Kang, J.; Huang, H.-Y.; et al. Epitranscriptomic Modification of MicroRNA Increases Atherosclerosis Susceptibility. *Circulation* **2023**, *148*, 1819–1822. [CrossRef]
100. Berliner, J.A.; Navab, M.; Fogelman, A.M.; Frank, J.S.; Demer, L.L.; Edwards, P.A.; Watson, A.D.; Lusis, A.J. Atherosclerosis—Basic Mechanisms—Oxidation, Inflammation, and Genetics. *Circulation* **1995**, *91*, 2488–2496. [CrossRef]
101. Yin, R.-X.; Yang, D.-Z.; Wu, J.-Z. Nanoparticle Drug-and Gene-eluting Stents for the Prevention and Treatment of Coronary Restenosis. *Theranostics* **2014**, *4*, 175–200. [CrossRef]
102. Mazighi, M.; Saint Maurice, J.P.; Bresson, D.; Szatmary, Z.; Houdart, E. Platelet Aggregation in Intracranial Stents May Mimic In-Stent Restenosis. *Am. J. Neuroradiol.* **2010**, *31*, 496–497. [CrossRef]
103. Kim, Y.; Weissler, E.H.; Pack, N.; Latz, C.A. A Systematic Review of Clopidogrel Resistance in Vascular Surgery: Current Perspectives and Future Directions. *Ann. Vasc. Surg.* **2023**, *91*, 257–265. [CrossRef] [PubMed]
104. Notarangelo, M.F.; Marziliano, N.; Giacalone, R.; Demola, M.A.; Conte, G.; Mantovani, F.; Ardissino, D. Stent thrombosis and clopidogrel response variability: Is the genetic test useful in clinical practice? *Giornale italiano di cardiologia (2006)* **2011**, *12*, 686–689. [PubMed]
105. Rogers, C.; Parikh, S.; Seifert, P.; Edelman, E.R. Endogenous cell seeding—Remnant endothelium after stenting enhances vascular repair. *Circulation* **1996**, *94*, 2909–2914. [CrossRef] [PubMed]
106. Liu, S.; Yang, Y.; Jiang, S.; Tang, N.; Tian, J.; Ponnusamy, M.; Tariq, M.A.; Lian, Z.; Xin, H.; Yu, T. Understanding the role of non-coding RNA (ncRNA) in stent restenosis. *Atherosclerosis* **2018**, *272*, 153–161. [CrossRef]
107. Sigwart, U.; Puel, J.; Mirkovitch, V.; Joffre, F.; Kappenberger, L. Intravascular Stents to Prevent Occlusion and Restenosis after Trans-Luminal Angioplasty. *New Engl. J. Med.* **1987**, *316*, 701–706. [CrossRef]
108. Haine, S.E.F.; Vrints, C.J.M. Stent thrombosis with drug-eluting and bare-metal stents. *Lancet* **2012**, *380*, 646. [CrossRef]
109. Kirtane, A.J.; Gupta, A.; Iyengar, S.; Moses, J.W.; Leon, M.B.; Applegate, R.; Brodie, B.; Hannan, E.; Harjai, K.; Jensen, L.O.; et al. Safety and Efficacy of Drug-Eluting and Bare Metal Stents Comprehensive Meta-Analysis of Randomized Trials and Observational Studies. *Circulation* **2009**, *119*, 3198–3206. [CrossRef]
110. Hu, W.; Jiang, J. Hypersensitivity and in-stent restenosis in coronary stent materials. *Front. Bioeng. Biotechnol.* **2022**, *10*, 1003322. [CrossRef]
111. Lansky, A.; Grubman, D.; Scheller, B. Paclitaxel-coated balloons: A safe alternative to drug-eluting stents for coronary in-stent restenosis. *Eur. Heart J.* **2020**, *41*, 3729–3731. [CrossRef]
112. Fu, C.; Li, Q.; Li, M.; Zhang, J.; Zhou, F.; Li, Z.; He, D.; Hu, X.; Ning, X.; Guo, W.; et al. An Integrated Arterial Remodeling Hydrogel for Preventing Restenosis After Angioplasty. *Adv. Sci.* **2024**, *11*, 2307063. [CrossRef]
113. Garg, S.; Serruys, P.W. Coronary Stents Current Status. *J. Am. Coll. Cardiol.* **2010**, *56*, S1–S42. [CrossRef] [PubMed]
114. Shen, Y.; Yu, X.; Cui, J.; Yu, F.; Liu, M.; Chen, Y.; Wu, J.; Sun, B.; Mo, X. Development of Biodegradable Polymeric Stents for the Treatment of Cardiovascular Diseases. *Biomolecules* **2022**, *12*, 1245. [CrossRef] [PubMed]
115. Hou, L.-D.; Li, Z.; Pan, Y.; Sabir, M.; Zheng, Y.-F.; Li, L. A review on biodegradable materials for cardiovascular stent application. *Front. Mater. Sci.* **2016**, *10*, 238–259. [CrossRef]
116. Seo, T.; Lafont, A.; Choi, S.-Y.; Barakat, A.I. Drug-Eluting Stent Design is a Determinant of Drug Concentration at the Endothelial Cell Surface. *Ann. Biomed. Eng.* **2016**, *44*, 302–314. [CrossRef]
117. Sun, X.; Li, H.; Qi, L.; Wang, F.; Hou, Y.; Li, J.; Guan, S. Construction and biocompatibility evaluation of MOF/S-HA composite coating on the surface of magnesium alloy vascular stent. *Prog. Org. Coat.* **2024**, *187*, 108177, Erratum in *Prog. Org. Coat.* **2024**, *189*, 108220. [CrossRef]
118. Udriste, A.S.; Burdusel, A.C.; Niculescu, A.-G.; Radulescu, M.; Grumezescu, A.M. Coatings for Cardiovascular Stents-An Up-to-Date Review. *Int. J. Mol. Sci.* **2024**, *25*, 1078. [CrossRef]
119. Marei, I.; Ahmetaj-Shala, B.; Triggle, C.R. Biofunctionalization of cardiovascular stents to induce endothelialization: Implications for in- stent thrombosis in diabetes. *Front. Pharmacol.* **2022**, *13*, 982185. [CrossRef]
120. Cornelissen, A.; Vogt, F.J. The effects of stenting on coronary endothelium from a molecular biological view: Time for improvement? *J. Cell. Mol. Med.* **2019**, *23*, 39–46. [CrossRef]
121. Cheng, H.; Zhao, Y.; Wang, Y.; Hou, Y.; Zhang, R.; Zong, M.; Sun, L.; Liu, Y.; Qi, J.; Wu, X.; et al. The Potential of Novel Synthesized Carbon Dots Derived Resveratrol Using One-Pot Green Method in Accelerating in vivo Wound Healing. *Int. J. Nanomed.* **2023**, *18*, 6813–6828. [CrossRef]
122. Zheng, S.; Tian, Y.; Ouyang, J.; Shen, Y.; Wang, X.; Luan, J. Carbon nanomaterials for drug delivery and tissue engineering. *Front. Chem.* **2022**, *10*, 990362. [CrossRef]
123. Huang, L.; Lyu, C.; Li, X.; Tang, G.; You, F.; Zhang, M.; Liu, F.; Jiang, X. Research progress on preparation, surface modification and application of carbon quantum dots. *J. Funct. Mater.* **2023**, *54*, 4045–4053.

124. Das, S.; Mondal, S.; Ghosh, D. Carbon quantum dots in bioimaging and biomedicines. *Front. Bioeng. Biotechnol.* **2024**, *11*, 1333752. [CrossRef] [PubMed]
125. Yuan, D.; Wang, P.; Yang, L.; Quimby, J.L.; Sun, Y.-P. Carbon "quantum" dots for bioapplications. *Exp. Biol. Med.* **2022**, *247*, 300–309. [CrossRef] [PubMed]
126. Shabbir, H.; Csapo, E.; Wojnicki, M. Carbon Quantum Dots: The Role of Surface Functional Groups and Proposed Mechanisms for Metal Ion Sensing. *Inorganics* **2023**, *11*, 262. [CrossRef]
127. Zhao, D.L.; Das, S.; Chung, T.-S. Carbon Quantum Dots Grafted Antifouling Membranes for Osmotic Power Generation via Pressure-Retarded Osmosis Process. *Environ. Sci. Technol.* **2017**, *51*, 14016–14023. [CrossRef]
128. Deng, Y.H.; Chen, J.H.; Yang, Q.; Zhuo, Y.Z. Carbon quantum dots (CQDs) and polyethyleneimine (PEI) layer-by-layer (LBL) self-assembly PEK-C-based membranes with high forward osmosis performance. *Chem. Eng. Res. Des.* **2021**, *170*, 423–433. [CrossRef]
129. Wang, Q.; Huang, J.; Sun, H.; Zhang, K.-Q.; Lai, Y. Uniform carbon dots@TiO_2 nanotube arrays with full spectrum wavelength light activation for efficient dye degradation and overall water splitting. *Nanoscale* **2017**, *9*, 16046–16058. [CrossRef]
130. Drachman, D.E.; Simon, D.I. Inflammation as a mechanism and therapeutic target for in-stent restenosis. *Curr. Atheroscler. Rep.* **2005**, *7*, 44–49. [CrossRef]
131. Pelliccia, F.; Zimarino, M.; Niccoli, G.; Morrone, D.; De Luca, G.; Miraldi, F.; De Caterina, R. In-stent restenosis after percutaneous coronary intervention: Emerging knowledge on biological pathways. *Eur. Heart J. Open* **2023**, *3*, oead083. [CrossRef]
132. Wen, L.; Qiu, H.; Li, S.; Huang, Y.; Tu, Q.; Lyu, N.; Mou, X.; Luo, X.; Zhou, J.; Chen, Y.; et al. Vascular stent with immobilized anti-inflammatory chemerin 15 peptides mitigates neointimal hyperplasia and accelerates vascular healing. *Acta Biomater.* **2024**, *179*, 371–384. [CrossRef]
133. Seegren, P.V.; Harper, L.R.; Downs, T.K.; Zhao, X.-Y.; Viswanathan, S.B.; Stremska, M.E.; Olson, R.J.; Kennedy, J.; Ewald, S.E.; Kumar, P.; et al. Reduced mitochondrial calcium uptake in macrophages is a major driver of inflammaging. *Nat. Aging* **2023**, *3*, 796–812. [CrossRef] [PubMed]
134. Hou, H.; Er, P.; Cheng, J.; Chen, X.; Ding, X.; Wang, Y.; Chen, X.; Yuan, Z.; Pang, Q.; Wang, P.; et al. High expression of FUNDC1 predicts poor prognostic outcomes and is a promising target to improve chemoradiotherapy effects in patients with cervical cancer. *Cancer Med.* **2017**, *6*, 1871–1881. [CrossRef] [PubMed]
135. Cui, Q.; Wen, S.; Huang, P. Targeting cancer cell mitochondria as a therapeutic approach: Recent updates. *Future Med. Chem.* **2017**, *9*, 929–949. [CrossRef] [PubMed]
136. Gao, X.; Schoettker, B. Reduction-oxidation pathways involved in cancer development: A systematic review of literature reviews. *Oncotarget* **2017**, *8*, 51888–51906. [CrossRef] [PubMed]
137. Yang, D.; Li, L.; Cao, L.; Chang, Z.; Mei, Q.; Yan, R.; Ge, M.; Jiang, C.; Dong, W.-F. Green Synthesis of Lutein-Based Carbon Dots Applied for Free-Radical Scavenging within Cells. *Materials* **2020**, *13*, 4146. [CrossRef]
138. Qiang, R.; Huang, H.; Chen, J.; Shi, X.; Fan, Z.; Xu, G.; Qiu, H. Carbon Quantum Dots Derived from Herbal Medicine as Therapeutic Nanoagents for Rheumatoid Arthritis with Ultrahigh Lubrication and Anti-inflammation. *Acs Appl. Mater. Interfaces* **2023**, *15*, 38653–38664. [CrossRef]
139. Zhao, Y.; Dai, E.; Dong, L.; Yuan, J.; Zhao, Y.; Wu, T.; Kong, R.; Li, M.; Wang, S.; Zhou, L.; et al. Available and novel plant-based carbon dots derived from Vaccaria Semen carbonisata alleviates liver fibrosis. *Front. Mol. Biosci.* **2023**, *10*, 1282929. [CrossRef]
140. Lu, F.; Yang, S.; Song, Y.; Zhai, C.; Wang, Q.; Ding, G.; Kang, Z. Hydroxyl functionalized carbon dots with strong radical scavenging ability promote cell proliferation. *Mater. Res. Express* **2019**, *6*, 065030. [CrossRef]
141. Chavez, J.; Khan, A.; Watson, K.R.; Khan, S.; Si, Y.; Deng, A.Y.; Koher, G.; Anike, M.S.; Yi, X.; Jia, Z. Carbon Nanodots Inhibit Tumor Necrosis Factor-α-Induced Endothelial Inflammation through Scavenging Hydrogen Peroxide and Upregulating Antioxidant Gene Expression in EA.hy926 Endothelial Cells. *Antioxidants* **2024**, *13*, 224. [CrossRef]
142. Li, S.; Guo, Z.; Zhang, Y.; Xue, W.; Liu, Z. Blood Compatibility Evaluations of Fluorescent Carbon Dots. *Acs Appl. Mater. Interfaces* **2015**, *7*, 19153–19162. [CrossRef]
143. Fedel, M.; Motta, A.; Maniglio, D.; Migliaresi, C. Carbon Coatings for Cardiovascular Applications: Physico-Chemical Properties and Blood Compatibility. *J. Biomater. Appl.* **2010**, *25*, 57–74. [CrossRef] [PubMed]
144. Koklic, T.; Majumder, R.; Lentz, B.R. Ca^{2+} switches the effect of PS-containing membranes on Factor Xa from activating to inhibiting: Implications for initiation of blood coagulation. *Biochem. J.* **2014**, *462*, 591–601. [CrossRef] [PubMed]

145. Yue, J.; Li, L.; Cao, L.; Zan, M.; Yang, D.; Wang, Z.; Chang, Z.; Mei, Q.; Miao, P.; Dong, W.-F. Two-Step Hydrothermal Preparation of Carbon Dots for Calcium Ion Detection. *Acs Appl. Mater. Interfaces* **2019**, *11*, 44566–44572. [CrossRef] [PubMed]
146. Fang, M.; Wang, B.; Qu, X.; Li, S.; Huang, J.; Li, J.; Lu, S.; Zhou, N. State-of-the-art of biomass-derived carbon dots: Preparation, properties, and applications. *Chin. Chem. Lett.* **2024**, *35*, 108423. [CrossRef]
147. Ridha, A.A.; Pakravan, P.; Azandaryani, A.H.; Zhaleh, H. Carbon dots; the smallest photoresponsive structure of carbon in advanced drug targeting. *J. Drug Deliv. Sci. Technol.* **2020**, *55*, 101408. [CrossRef]
148. Bartkowski, M.; Zhou, Y.; Nabil Amin Mustafa, M.; Eustace, A.J.; Giordani, S. CARBON DOTS: Bioimaging and Anticancer Drug Delivery. *Chem.-A Eur. J.* **2024**, *30*, e202303982. [CrossRef]
149. Kaurav, H.; Verma, D.; Bansal, A.; Kapoor, D.N.; Sheth, S. Progress in drug delivery and diagnostic applications of carbon dots: A systematic review. *Front. Chem.* **2023**, *11*, 1227843. [CrossRef]
150. Yuan, Y.; Guo, B.; Hao, L.; Liu, N.; Lin, Y.; Guo, W.; Li, X.; Gu, B. Doxorubicin-loaded environmentally friendly carbon dots as a novel drug delivery system for nucleus targeted cancer therapy. *Colloids Surf. B-Biointerfaces* **2017**, *159*, 349–359. [CrossRef]
151. Dong, X.; Liang, W.; Meziani, M.J.; Sun, Y.-P.; Yang, L. Carbon Dots as Potent Antimicrobial Agents. *Theranostics* **2020**, *10*, 671–686. [CrossRef]
152. Calabrese, G.; De Luca, G.; Nocito, G.; Rizzo, M.G.; Lombardo, S.P.; Chisari, G.; Forte, S.; Sciuto, E.L.; Conoci, S. Carbon Dots: An Innovative Tool for Drug Delivery in Brain Tumors. *Int. J. Mol. Sci.* **2021**, *22*, 11783. [CrossRef]
153. Zhao, F.; Liu, F.; Gao, C.; Wang, G.; Zhang, Y.; Yu, F.; Tian, J.; Tan, K.; Zhang, R.; Liang, K.; et al. Interfacing exogenous stents with human coronary artery by self-assembled coating: Designs, functionalities and applications. *NPG Asia Mater.* **2024**, *16*, 28. [CrossRef]
154. Raikar, A.S.; Priya, S.; Bhilegaonkar, S.P.; Somnache, S.N.; Kalaskar, D.M. Surface Engineering of Bioactive Coatings for Improved Stent Hemocompatibility: A Comprehensive Review. *Materials* **2023**, *16*, 6940. [CrossRef] [PubMed]
155. Tajik, S.; Dourandish, Z.; Zhang, K.; Beitollahi, H.; Le, Q.V.; Jang, H.W.; Shokouhimehr, M. Carbon and graphene quantum dots: A review on syntheses, characterization, biological and sensing applications for neurotransmitter determination. *Rsc Adv.* **2020**, *10*, 15406–15429. [CrossRef] [PubMed]
156. Thota, S.P.; Kolli, N.K.; Kurdekar, A.; Thota, S.M.; Vadlani, P.V.; Kumar, B.S. One-step synthesis of biocompatible luminescent carbon dots from Cuscuta for bio-imaging application. *Biomass Convers. Biorefinery* **2023**, *13*, 1–8. [CrossRef]
157. Wang, Q.; Wang, R.; Zhang, Q.; Zhao, C.; Zhou, X.; Zheng, H.; Zhang, R.; Sun, Y.; Yan, Z. Application of Biomass Corrosion Inhibitors in Metal Corrosion Control: A Review. *Molecules* **2023**, *28*, 2832. [CrossRef]
158. Fan, Y.; Zhang, Y.; Yin, L.; Zhao, C.; He, Y.; Zhang, C. Research Progress on Carbon Dots in Field of Metal Corrosion and Protection. *J. Chin. Soc. Corros. Prot.* **2023**, *43*, 1237–1246.
159. Cao, S.; Liu, D.; Wang, T.; Ma, A.; Liu, C.; Zhuang, X.; Ding, H.; Mamba, B.B.; Gui, J. Nitrogen-doped carbon dots as high-effective inhibitors for carbon steel in acidic medium. *Colloids Surf. A-Physicochem. Eng. Asp.* **2021**, *616*, 126280. [CrossRef]
160. Liao, J.; Chu, Q.; Zhao, S.; Liu, Z.; Zhang, X. Recent advances in carbon dots as powerful ecofriendly corrosion inhibitors for copper and its alloy. *Mater. Today Sustain.* **2024**, *26*, 100706. [CrossRef]
161. Padhan, S.; Rout, T.K.; Nair, U.G. N-doped and Cu,N-doped carbon dots as corrosion inhibitor for mild steel corrosion in acid medium. *Colloids Surf. A-Physicochem. Eng. Asp.* **2022**, *653*, 129905. [CrossRef]
162. Zhou, S.; Liu, Z.; Lu, Z.; Ma, L. Carbon dot/nickel nanocomposite coating for wear and corrosion control of Mg alloy: Experimental and theoretical studies. *Appl. Surf. Sci.* **2024**, *659*, 159845. [CrossRef]
163. Darani, M.K.; Rouhani, S.; Ranjbar, Z. Carbon dot enhanced electrodeposited coatings for advanced early-stage corrosion sensing. *Opt. Mater.* **2024**, *154*, 115771. [CrossRef]
164. Ma, L.; Zhou, S. Preparation Method of Nickel Coating Doped with Nanoparticles on Magnesium Alloy. CN117646265A, 5 March 2024.
165. Bilas, P.; Nomede-Martyr, N.; Mathieu, G.; Bercion, Y.; Cesaire, T.; Thomas, P. Tribological properties of Sargassum carbon dots as additives in water-based lubricants. *Mater. Lett.* **2024**, *354*, 135411. [CrossRef]
166. Wang, H.; Li, Y.; Zhang, S.; Che, Q.; Hu, L.; Zhang, J. Excellent corrosion inhibition and lubrication properties of carbon dot-based ionic liquids as water-based additives. *Tribol. Int.* **2023**, *189*, 108990. [CrossRef]
167. Chimeno-Trinchet, C.; Pacheco, M.E.; Fernandez-Gonzalez, A.; Diaz-Garcia, M.E.; Badia-Laino, R. New metal-free nanolubricants based on carbon-dots with outstanding antiwear performance. *J. Ind. Eng. Chem.* **2020**, *87*, 152–161. [CrossRef]
168. Mou, Z.; Yang, Q.; Peng, J.; Yan, R.; Zhao, B.; Ge, Y.; Xiao, D. One-step green synthesis of oil-dispersible carbonized polymer dots as eco-friendly lubricant additives with superior dispersibility, lubricity, and durability. *J. Colloid Interface Sci.* **2022**, *623*, 762–774. [CrossRef]
169. Duarah, R.; Singh, Y.P.; Gupta, P.; Mandal, B.B.; Karak, N. High performance bio-based hyperbranched polyurethane/carbon dot-silver nanocomposite: A rapid self-expandable stent. *Biofabrication* **2016**, *8*, 045013. [CrossRef]
170. Mahmud, Z.; Nasrin, A.; Hassan, M.; Gomes, V.G. 3D-printed polymer nanocomposites with carbon quantum dots for enhanced properties and in situ monitoring of cardiovascular stents. *Polym. Adv. Technol.* **2022**, *33*, 980–990. [CrossRef]
171. Chauhan, P.; Mundekkad, D.; Mukherjee, A.; Chaudhary, S.; Umar, A.; Baskoutas, S. Coconut Carbon Dots: Progressive Large-Scale Synthesis, Detailed Biological Activities and Smart Sensing Aptitudes towards Tyrosine. *Nanomaterials* **2022**, *12*, 162. [CrossRef]

172. Sajjad, F.; Han, Y.; Bao, L.; Yan, Y.; Shea, D.O.; Wang, L.; Chen, Z. The improvement of biocompatibility by incorporating porphyrins into carbon dots with photodynamic effects and pH sensitivities. *J. Biomater. Appl.* **2022**, *36*, 1378–1389. [CrossRef]
173. Feng, B.; Li, N.; Bi, Y.; Kong, F.; Wang, Z.; Tan, S. Bio-based Carbon dots Loaded with 5-Fu: A Multifunctional drug Delivery System. *J. Fluoresc.* **2024**, *34*, 1683–1692. [CrossRef]